

# Reaching the speed limit of classical block ciphers via quantum-like operator spreading

Claudio Chamon,<sup>1</sup> Eduardo R. Mucciolo,<sup>2</sup> and Andrei E. Ruckenstein<sup>1</sup>

<sup>1</sup>*Physics Department, Boston University, Boston, Massachusetts 02215, USA*

<sup>2</sup>*Department of Physics, University of Central Florida, Orlando, Florida 32816, USA*

(Dated: November 16, 2020)

We cast encryption via classical block ciphers in terms of operator spreading in a dual space of Pauli strings, a formulation which allows us to characterize classical ciphers by using tools well known in the analysis of quantum many-body systems. We connect plaintext and ciphertext attacks to out-of-time order correlators (OTOCs) and quantify the quality of ciphers using measures of delocalization in string space such as participation ratios and corresponding entropies obtained from the wave function amplitudes in string space. In particular, we show that in Feistel ciphers the entropy saturates its bound to exponential precision for ciphers with 4 or more rounds, consistent with the classic Luby-Rackoff result that it takes these many rounds to generate strong pseudo-random permutations. The saturation of the string-space information entropy is accompanied by the vanishing of OTOCs. Together these signal irreversibility and chaos, which we take to be the defining properties of good classical ciphers. More precisely, we define a good cipher by requiring that the saturation of the entropy and the vanishing of OTOCs occurs to super-polynomial precision, implying that the cipher cannot be distinguished from a pseudorandom permutation with a polynomial number of queries. We argue that this criterion can be satisfied by  $n$ -bit block ciphers implemented via random reversible circuits with  $\mathcal{O}(n \log n)$  gates. These circuits - which we refer to as long-ranged packed circuits - are composed of layers of  $n/3$  non-overlapping non-local random 3-bit gates. We show that in order to reach this “speed limit” one must employ a two-stage circuit: the first stage deploys a special set of linear “inflationary” gates that accelerate the growth of small individual strings; followed by a second stage implemented via universal gates that exponentially proliferate the number of macroscopic strings. The close formal correspondence to quantum scramblers established in this work leads us to suggest that this two-stage construction is also required in order to scramble quantum states to similar precision and with circuits of similar size.

## I. INTRODUCTION

A block cipher encrypts a plaintext message, broken up into a series of blocks of bits, by mapping it into ciphertext blocks of the same size [1]. The development of algorithms that implement “good” block ciphers usually involves constructing pseudorandom permutations through an iterative process which scrambles the initial plaintext. Notable examples are: (1) Feistel ciphers [1, 2], which use pseudorandom functions to build pseudorandom permutations through multiple rounds of shuffles and toggles of bit-registers; and (2) random compositions of small permutations on, at a minimum, 3 bits at a time [3–5]. In this paper we use the latter framework of random classical circuits built from universal 3-bit gates to explore classical ciphers from a new point of view. In particular, we formulate plaintext or ciphertext attacks, which can be cast as combinations of flipping and/or measuring strings of bits, in terms of out-of-time-order correlators (OTOCs) of string operators representing the attacks. In our specific context, the security of a block cipher translates into the exponential decay of OTOCs as a function of “computational” time, behavior which in quantum systems signals the approach to a chaotic state [6–12].

The principal conclusion of this paper, which we reach through a combination of analytical and numerical arguments, is that one can build classical block ciphers on  $n$  bits, secure to polynomial attacks, with as few as

$\mathcal{O}(n \log n)$  gates in circuits of depth  $\mathcal{O}(\log n)$ . We believe that this result, as well as the physics inspired approach proposed in this paper, should have important implications to many cryptographic applications, especially those requiring fast rates of encryption when dealing with large data sets.

The important conceptual element of this paper is to map strings of Pauli operators describing classical attacks into a dual quantum mechanical space of strings in which the evolution of string operators is translated into evolution in a Hilbert space of strings. Within this string picture, the computation implemented by universal classical gates evolves an initial string into a *superposition* of string states. The special feature which makes the quantum mechanical analogy non-trivial is the presence of non-linear classical gates  $g$  in bit space [ i.e., those for which  $g(x \oplus y) \neq g(x) \oplus g(y) \oplus c$ , for constant  $c$  ]. It is this non-linearity that leads to the proliferation of string components making up the quantum superposition, by contrast with linear gates, which can only change the state of a single string. Thus, as a result of evolution via non-linear gates, the string wave function spreads over the full Hilbert space of strings, reaching an asymptotic state that cannot be distinguished from a random wave function drawn from an ensemble that respects all the symmetries of the system. It is the closeness to this asymptotic state that measures the quality of the classical cipher, and it is the evolution towards this state that

defines the speed of the scrambling process.

Here we quantify the delocalization of the wave function in string space in terms of generalized inverse participation ratios [13], and corresponding entropies. In the asymptotic state, these entropies reach their maximum values, which include a universal correction of order 1 that only depends on the symmetries of the wave functions, as we illustrate through a comparison between classical circuits built from 3-bit permutation gates in  $S_8$  and quantum circuits of 2-qubit gates in either  $U(4)$  or  $O(4)$ . The discrete or continuous, real or complex nature of the wave function in string space is preserved under evolution, defining three distinct symmetry classes: permutation, orthogonal, and unitary. Moreover, the asymptotic-state OTOCs vanish, which together with the maximum entropy reflect the chaotic and irreversible nature of the evolution.

We view the residual entropy – the difference from the maximum entropy – as the measure of how much information can be extracted by an adversary. We illustrate this principle by computing the entropies for a Feistel cipher as function of the number of rounds. We show that: (a) for 1 or 2 rounds the entropy differs by an extensive amount from the maximum; (b) for 4 or more rounds the entropy reaches its maximum up to exponentially-small finite-size corrections; and (c) for 3 rounds the entropy reaches its extensive maximum but with an order 1 deficit with respect to the universal (order 1) correction. These results are consistent with the conclusions of the classic Luby-Rackoff work [2], and reflect the fact that a Feistel cipher with 4 or more rounds yields a strong-pseudorandom permutation, while a 3-round cipher is “marginal” in that a combined 3-query plaintext/ciphertext attack (that exploits the regular structure of the alternating left/right rounds of the Feistel cipher) can distinguish the resulting permutation from a strong-pseudorandom one [14]. Equivalently, the 3-string OTOC associated to this attack vanishes, and thus signals chaotic behavior, only for 4 or more rounds.

Arguably, the main contribution of this paper is to determine, for a cipher built via random reversible classical circuits, the minimum number of 3-bit gates needed to reach the asymptotic random multi-string wave function. Physically, the evolution to this asymptotic state occurs through quantum diffusion in string space, controlled by transition amplitudes between string states induced by the action of the gates in bit space. We study the statistics of these transition amplitudes and their associated transition probabilities for the case of interest, the 3-bit permutation gates, and compare it to the cases of 2-qubit quantum orthogonal and unitary gates. As shown explicitly in this paper, the essential feature in all three symmetry classes is that the evolution via universal gates leads to string proliferation due to non-zero matrix elements between an initial string state and multiple final states.

As already mentioned above, we find that the minimum size circuit leading to the vanishing of both the residual entropy and OTOCs is within super-polynomial

precision scales as  $\mathcal{O}(n \log n)$ . In the context of the cipher, this implies that the action of a random circuit of this size cannot be distinguished from a pseudorandom permutation with a polynomial number of queries. Establishing this result requires eliminating a bottleneck associated with the probability that small initial strings do not grow sufficiently fast. This bottleneck occurs because the evolution through generic gates results in a non-zero stay-probability  $p$  for size (or weight) 1 substrings; which, in turn, translates into a tail in the distribution of string sizes that scales as  $p^\ell$  after the application of  $\ell$  layers of  $n/3$  non-overlapping 3-bit gates. These tails contribute undesirable polynomial corrections to both the residual entropy and OTOCs for  $\ell \sim \log n$ . We eliminate these tails by structuring the circuit so as to separate two distinct processes: (a) the extension of a small weight string in the initial state to a string of macroscopic weight; and (b) the splitting of the resulting macroscopic string into a superposition of exponentially many string states, a process necessary for the decay of the residual entropy and the OTOCs. The first “inflation” stage is a circuit built by drawing from a set of 144 special linear gates (out of the  $8!$  3-bit permutation gates) for which the stay-probability for weight 1 substrings vanishes. In bit space, these gates flip two or more bits at the output when a single bit is flipped at the input. We show that the use of these gates allows us to reach macroscopic size strings with  $\ell \sim \log n$  or, equivalently, with a circuit of  $\mathcal{O}(n \log n)$  gates. The inflation stage is followed by a second “proliferation/equilibration” stage that uses the full set of linear and non-linear 3-bit gates. During this stage the entropy and the OTOCs decay exponentially with the number of applied layers. We show that the decay rate depends on how the circuit is structured: for circuits with short-range gates acting on nearest-neighbor bits in 1-, 2-, and 3-dimensional lattices, the decay rate with  $\ell$  is independent of the number of bits  $n$ ; for random circuits of long-range 3-bit gates acting on any triplet of bits and covering all  $n$  bits in every layer of  $n/3$  gates, we find that the decay rate depends on the number of bits and is accelerated by a factor scaling logarithmically in  $n$ . This logarithmic scaling implies that for long-range circuits the entropy and the OTOCs vanish to super-polynomial order for  $\ell \sim \log n$  or, equivalently, with a circuit of  $\mathcal{O}(n \log n)$  gates, the same scaling form required in the first stage. Thus the two-stage implementation with the random long-range packed circuit (i.e., built out of layers of  $n/3$  non-overlapping 3-bit gates) reaches a cipher that cannot be distinguished from a pseudorandom permutation with a polynomial number of queries within  $\mathcal{O}(n \log n)$  gates.

We should stress that the mapping to string space highlights a connection between classical ciphers and the problem of scrambling by random quantum circuits [15–20]. This problem has engendered a great deal of interest in the context of the recent demonstration of quantum supremacy [21], as well as in studies of information processing in black holes, which are

conjectured to be the fastest scramblers in nature [8–10, 12, 22, 23]. In the case of random quantum circuits, resolving the bottleneck associated with the growth of small strings that we mentioned above, requires circuits of sizes  $\mathcal{O}(n \log^2 n)$  [17, 18, 20]. Our work suggests that, as in the classical cipher, one can further reduce the circuit size to  $\mathcal{O}(n \log n)$  gates in the quantum case by deploying the two-stage construction described here. It remains to be determined whether the inflationary period can be implemented via the unstructured (i.e., random) placement of 2-qubit gates or it requires using our 144 linear 3-bit gates or their circuit-equivalent built from the correlated placement of 2-qubit CNOT gates.

Finally, we expect that ciphers based on random circuits are immune to quantum attacks. Known vulnerabilities to such attacks arise as a result of periodicities induced by design regularities, such as the right/left structure of rounds in Feistel ciphers [24], regularities that are absent in both classical and quantum random circuits.

The plan of the paper is as follows: in section II we introduce notation and formulate classical ciphers and general attacks in terms of OTOCs, the vanishing of which establish a criterium for cipher security. With the notation and formal framework in place, we are in position to summarize our key conceptual contributions in section III, setting up the roadmap for the rest of the paper. In section IV we formulate the dynamics of the Pauli operators entering the OTOCs as a quantum evolution problem in a dual string space. In subsection IV A, we introduce generalized inverse participation ratios and their associated entropies for quantifying the delocalization of the wave function in string space. In section V we derive the equilibrium distribution for the string wave function amplitudes for random permutations, and compare with those obtained for random unitary and orthogonal transformations, and extract bounds on the entropies for all three symmetry classes (see subsection V C). Subsection V B focuses on the case of permutations and uses entropies as diagnostics for the security of Feistel ciphers, providing a direct connection to the well-known results of Luby and Rackoff [2]. In subsection V D we establish the vanishing of OTOC in the equilibrium state characterized by independently and identically distributed string amplitudes,  $A_{\beta\alpha}$ . We turn to the dynamics of the approach to the asymptotic equilibrium state in subsection VI, where we emphasize the common origin of string spreading in the structure of the string-space transition matrix elements for the three symmetry classes of gates, and argue for the same universal scaling of the minimum size circuit and the equilibration times for classical and quantum circuits. Subsection VI A introduces a mean field analysis of the OTOC corresponding to the avalanche criterium, which encodes the fact that in a secure cipher flipping a single bit in the input flips half of the bits in the output. The mean field treatment describes accurately average properties for the case of a circuit of long-range (but not packed) random gates. In the same section we discuss the subtlety connected with

long tails in the distribution of string weights that slow down scrambling by both classical and quantum random circuits. In subsection VIB we introduce the two stage circuit which eliminates the polynomial tails connected with short strings, and present numerical evidence that random long-range packed circuits provide an implementation of classical ciphers secure to polynomial attacks with as few as  $\mathcal{O}(n \ln n)$  gates. The paper ends in section VII with concluding remarks and questions for future research.

## II. BLOCK CIPHERS AND REVERSIBLE COMPUTATION

A block cipher is a permutation,  $P$ , that acts on the space of binary states of  $n$  bits, i.e.,  $P$  is an element of the symmetric group  $S_{2^n}$ . Permutations can be thought of as reversible classical computations, which can be encoded in circuits of universal reversible gates acting on a small number of bits. More precisely, even permutations can be decomposed into products of small permutations (elements of  $S_8$ ) acting on 3 bits at a time, as shown by Coppersmith and Grossman [3]. (The realization of odd permutations requires either one additional  $n$ -bit gate or one ancilla bit.) These small permutations can be represented using a set of universal reversible gates, for example NOT, CNOT, and Toffoli gates [25]; here we work directly with the small permutation gates in  $S_8$ .

### A. Notation

Hereafter we use quantum bracket notation, and represent a permutation  $P$  acting on a binary string  $x \in \{0, 1\}^n$  as an operator  $\hat{P}$  acting on a state  $|x\rangle \equiv |x_0 x_1 \dots x_{n-1}\rangle$ ,

$$\hat{P} |x\rangle = |P(x)\rangle. \quad (1)$$

The permutation operator  $\hat{P}$  is unitary and real:  $\hat{P}^{-1} = \hat{P}^\dagger = \hat{P}^\top$ .

In this representation, reading and flipping bits are implemented using the Pauli operators  $\hat{\sigma}_i^z$  and  $\hat{\sigma}_i^x$ , respectively:

$$\begin{aligned} \hat{\sigma}_i^z |x\rangle &= (-1)^{x_i} |x\rangle \\ \hat{\sigma}_i^x |x\rangle &= |x_0 x_1 \dots \bar{x}_i \dots x_{n-1}\rangle, \end{aligned} \quad (2)$$

where  $\bar{x}_i$  is the negation of  $x_i$ . We also introduce  $P_i(x)$  to denote the  $i$ -th bit of  $P(x)$ , which can be read via

$$\hat{P}^\top \hat{\sigma}_i^z \hat{P} |x\rangle = (-1)^{P_i(x)} |x\rangle. \quad (3)$$

Since the operator  $\hat{P}$  evolves the input state  $|x\rangle$  into the output state  $|P(x)\rangle$ , it is natural to interpret

$$\hat{\sigma}_i^z(\tau) \equiv \hat{P}^\top \hat{\sigma}_i^z \hat{P} \quad (4)$$

as the Heisenberg evolution of the operator  $\hat{\sigma}_i^z$  in the course of the computation. Here  $\tau$  defines the accumulated “time” of the computation, which counts the number of gates of the circuit implementing the permutation  $P$ . More generally, we define  $\hat{O}(\tau) \equiv \hat{P}^\top \hat{O} \hat{P}$  as well as  $\hat{O}(0) \equiv \hat{O}$  which represent operators at the output and input ends of the cipher, respectively.

### B. Cryptanalysis via correlation functions

In the context of the quantum language defined above, a criterium for “good” ciphers will be expressed through the behavior of a class of correlation functions known as out-of-time-order correlators (OTOCs) [6–12]. Following cryptanalysis, we diagnose the quality of the ciphers in terms of plaintext and ciphertext attacks corresponding to arbitrary readouts and flips on both inputs and outputs.

Consider first a simple example of plaintext attack in which an adversary probes the sensitivity of the output bit  $j$  to flipping an input bit  $i$ , as expressed by

$$C_{\text{SAC}}^{ij} = \frac{1}{2^n} \sum_x (-1)^{P_j(x \oplus c_i) \oplus P_j(x)}, \quad (5)$$

with  $c_i = 2^i$  and the bitwise XOR operation for two  $n$ -bit strings  $x \oplus c_i$  implementing the flip of the  $i$ -th bit of  $x$ . The Strict Avalanche Criterium (SAC) test [26–28] requires that the function  $P_j(x \oplus c_i) \oplus P_j(x)$  is balanced, i.e., it is 0 or 1 with equal frequency, and thus  $C_{\text{SAC}}$  vanishes. For random permutations,  $C_{\text{SAC}}$  vanishes up

to corrections that are exponentially small in  $n$ . Notice that Eq. (5) requires summing over all  $2^n$  initial states  $x$ ; in a practical attack, only a number of samples  $M$  (polynomial in  $n$ ) is accessible, in which case an adversary cannot resolve  $C_{\text{SAC}}$  below a noise level of  $\mathcal{O}(1/\sqrt{M})$ .

Within the quantum notation, Eq. (5) can be cast as a correlation function,

$$\begin{aligned} C_{\text{SAC}}^{ij} &= \frac{1}{2^n} \sum_x \langle x | \hat{\sigma}_i^x(0) \hat{\sigma}_j^z(\tau) \hat{\sigma}_i^x(0) \hat{\sigma}_j^z(\tau) | x \rangle \\ &\equiv \text{tr} [\rho_\infty \hat{\sigma}_i^x(0) \hat{\sigma}_j^z(\tau) \hat{\sigma}_i^x(0) \hat{\sigma}_j^z(\tau)] , \end{aligned} \quad (6)$$

where  $\rho_\infty \equiv \mathbb{1}/2^n$  can be viewed as an infinite temperature density matrix. This correspondence is evidenced by following the sequence of operators from right-to-left in the first line of Eq. (6):

1.  $\hat{\sigma}_j^z(\tau)$  measures the value of the  $j$ -th bit,  $(-1)^{P_j(x)}$ , at the output and returns the system to the initial input state,  $|x\rangle$ ;
2.  $\hat{\sigma}_i^x(0)$  flips the  $i$ -th bit of the initial input state,  $|x\rangle$ , into  $|x \oplus c_i\rangle$ ;
3.  $\hat{\sigma}_j^z(\tau)$  measures the  $j$ -th bit,  $(-1)^{P_j(x \oplus c_i)}$ , at the output and returns the system to the input state  $|x \oplus c_i\rangle$ ; and finally,
4.  $\hat{\sigma}_i^x(0)$  flips the  $i$ -th bit back, returning the system to the initial state  $|x\rangle$ .

As a second more complex example, we consider an attack that distinguishes a Feistel cipher build via a 3-round Luby-Rackoff construction from a strong pseudorandom permutation. This cipher is vulnerable to a classical adaptive chosen plaintext and chosen ciphertext attack (CPCA) [14], involving three queries, which we translate into the following OTOC:

$$\begin{aligned} C_{\text{CPCA}}^{ij} &= \text{tr} [\rho_\infty \hat{\sigma}_j^x(0) \hat{\sigma}_i^x(\tau) \hat{\sigma}_i^z(0) \hat{\sigma}_i^x(\tau) \hat{\sigma}_j^z(\tau) \hat{\sigma}_j^x(0) \hat{\sigma}_j^z(\tau) \hat{\sigma}_i^z(0)] \\ &= (-1)^{\delta_{ij}} \text{tr} [\rho_\infty (\hat{\sigma}_i^z(0) \hat{\sigma}_i^x(\tau))^2 (\hat{\sigma}_j^z(\tau) \hat{\sigma}_j^x(0))^2] . \end{aligned} \quad (7)$$

We note that the 4-round version of this cipher is immune to this attack, as are ciphers based on sufficiently long random reversible circuits.

### III. SUMMARY OF CONCEPTUAL CONTRIBUTIONS

Having introduced the formal framework, we are in position to outline the four conceptual contributions of this paper. The first one is to represent any plaintext/ciphertext attack involving multiple readouts and/or flips of bits at both inputs and outputs in the form of an OTOC of Pauli string operators

$$\hat{S}_\alpha = \prod_{j \in \alpha^x} \hat{\sigma}_j^x \prod_{k \in \alpha^z} \hat{\sigma}_k^z , \quad (8)$$

namely

$$C_{\text{CPCA}}^{\alpha_1, \beta_1 \dots \alpha_k, \beta_k} = \text{tr} [\rho_\infty \hat{S}_{\alpha_1}(0) \hat{S}_{\beta_1}(\tau) \hat{S}_{\alpha_2}(0) \hat{S}_{\beta_2}(\tau) \dots \hat{S}_{\alpha_k}(0) \hat{S}_{\beta_k}(\tau)] . \quad (9)$$

A Pauli string is labeled by the set  $\alpha = (\alpha^x, \alpha^z)$  of bit indices present in the string. (We choose to place all the  $\hat{\sigma}^x$  operators to the left of the  $\hat{\sigma}^z$ 's<sup>1</sup>.)

The second conceptual contribution is to tie the security of the cipher to the vanishing of OTOCs representing plaintext/ciphertext attacks. In the quantum case, for both Hamiltonian systems and evolution via random quantum circuits, the vanishing of OTOCs is associated with irreversibility and chaos [7–12].

The third contribution is to connect the vanishing of OTOCs to the delocalization of the dual string-space wave function via the growth in size and exponential proliferation in number of Pauli strings in the course of the computation. We quantify this delocalization in terms of generalized inverse participation ratios [13] and corresponding entropies, which saturate for a random string wave function, thus tying together the vanishing of the OTOCs and the vanishing of the residual entropies.

Finally, the fourth contribution is to realize that one must break the circuit into two stages in order to construct a cipher with as few as  $\mathcal{O}(n \log n)$  gates for which the residual entropy and OTOCs vanish to super-polynomial precision.

#### IV. QUANTUM EVOLUTION IN STRING SPACE

The description of OTOCs in terms of strings in Eq. (9) brings out the connection to quantum mechanics that is critical to our analysis: time evolution leads to superpositions in string space. It is this correspondence that allows us to unify results in classical and quantum random circuits.

We further note that while classical permutations are the principal motivation for this work, below we use  $\hat{P}$  to denote a general unitary transformation, since in considering the connection to quantum computation  $\hat{P}$  will be replaced by a unitary  $\hat{U}$  or orthogonal  $\hat{O}$  transformation. The special properties of permutation operators will be noted as needed.

The connection to quantum mechanics is made manifest by translating the string operators  $\hat{S}_\beta$  and  $\hat{S}_\alpha^\dagger$  defined by Eq. (8) into bra  $\langle \beta |$  and ket  $| \alpha \rangle$  states in a dual string

space that inherits the inner product

$$\langle \beta | \alpha \rangle = \frac{1}{2^n} \text{tr} \left( \hat{S}_\beta \hat{S}_\alpha^\dagger \right) = \delta_{\beta\alpha} . \quad (10)$$

The states resulting from this operator-to-state correspondence should be viewed as tensor products of  $n$  qudits that label 4 possible Pauli operators at each position in the string. The Heisenberg evolution of the string operators

$$\hat{S}_\beta(\tau) \equiv \hat{P}^\dagger(\tau) \hat{S}_\beta \hat{P}(\tau) = \sum_\alpha A_{\beta\alpha}(\tau) \hat{S}_\alpha \quad (11)$$

corresponds to the evolution in Hilbert space of string states via the unitary operator  $\hat{U}_P$ , namely,

$$\langle \beta(\tau) | = \langle \beta | \hat{U}_P = \sum_\alpha A_{\beta\alpha}(\tau) \langle \alpha | , \quad (12)$$

with the transition amplitudes between the string states  $\alpha$  and  $\beta$  are given by

$$\begin{aligned} A_{\beta\alpha}(\tau) &= \langle \beta | \hat{U}_P | \alpha \rangle \\ &= \frac{1}{2^n} \text{tr} \left( \hat{P}^\dagger \hat{S}_\beta \hat{P} \hat{S}_\alpha^\dagger \right) . \end{aligned} \quad (13)$$

We note that if one breaks the operators  $\hat{P}$  and  $\hat{P}^\dagger$  above into gates, these appear sequentially bookending the operator  $\hat{S}_\beta$  in reverse-time order or, using the cyclic property of the trace, the operator  $\hat{S}_\alpha^\dagger$  in the natural time order. Thus, the amplitudes  $A_{\beta\alpha}(\tau)$  can be viewed as describing either forward propagation from  $\alpha$  to  $\beta$  or backward propagation from  $\beta$  to  $\alpha$ . Moreover  $A_{\beta\alpha}(\tau)$  satisfies the normalization conditions

$$\sum_\beta |A_{\beta\alpha}(\tau)|^2 = \sum_\alpha |A_{\beta\alpha}(\tau)|^2 = 1 , \quad (14)$$

which follow from the unitarity of  $\hat{U}_P$ , itself a consequence of preservation of the norm under time-evolution:

$$\begin{aligned} \langle \beta | \hat{U}_P \hat{U}_P^\dagger | \alpha \rangle &= \langle \beta(\tau) | \alpha(\tau) \rangle \\ &= \frac{1}{2^n} \text{tr} \left( \hat{P}^\dagger \hat{S}_\beta \hat{P} \hat{P}^\dagger \hat{S}_\alpha^\dagger \hat{P} \right) \\ &= \langle \beta | \alpha \rangle . \end{aligned} \quad (15)$$

Using the string amplitudes  $A_{\alpha\beta}$  we can re-express the OTOC in Eq. (9):

<sup>1</sup> By adding a phase  $i^{\alpha^x \cdot \alpha^z}$  to  $\hat{S}_\alpha$  – picking up an  $i$  each time both a  $\hat{\sigma}_j^x$  and  $\hat{\sigma}_j^z$  appear at the same  $j$ , or basically deploying the  $\hat{\sigma}^y$ 's as well – would make the string operator Hermitian. Here

we prefer the definition Eq. (8) for the applications we consider, and work explicitly with both  $\hat{S}_\alpha$  and  $\hat{S}_\alpha^\dagger$  when needed.

$$\begin{aligned}
C_{\text{CPCA}}^{\alpha_1, \beta_1 \dots \alpha_k, \beta_k} &= \sum_{\gamma_1, \dots, \gamma_k} A_{\beta_1 \gamma_1}(\tau) A_{\beta_2 \gamma_2}(\tau) \dots A_{\beta_k \gamma_k}(\tau) \text{tr} \left[ \rho_\infty \hat{S}_{\alpha_1} \hat{S}_{\gamma_1} \hat{S}_{\alpha_2} \hat{S}_{\gamma_2} \dots \hat{S}_{\alpha_k} \hat{S}_{\gamma_k} \right] \\
&= \sum_{\gamma_1, \dots, \gamma_k} A_{\beta_1 \gamma_1}(\tau) A_{\beta_2 \gamma_2}(\tau) \dots A_{\beta_k \gamma_k}(\tau) (-1)^{\sum_{i \leq j} \alpha_i^z \cdot \gamma_j^x} (-1)^{\sum_{i < j} \gamma_i^z \cdot \alpha_j^x} (-1)^{\sum_{i < j} \alpha_i^z \cdot \alpha_j^x} (-1)^{\sum_{i < j} \gamma_i^z \cdot \gamma_j^x} \\
&\quad \times \delta_{\alpha_1^x \oplus \dots \oplus \alpha_k^x, \gamma_1^x \oplus \dots \oplus \gamma_k^x} \delta_{\alpha_1^z \oplus \dots \oplus \alpha_k^z, \gamma_1^z \oplus \dots \oplus \gamma_k^z} .
\end{aligned} \tag{16}$$

where the  $\cdot$  product is defined as  $a \cdot b \equiv a_1 b_1 + \dots + a_n b_n$ . An important quantity that will be used throughout the paper is the string weight, defined as  $w(\alpha) \equiv \sum_i (\alpha_i^x \vee \alpha_i^z)$ , which measures the number of non-identity Pauli operators that compose the string. (Each  $\alpha_i^x \vee \alpha_i^z$  is 1 if at location  $i$  the string has an  $\hat{\sigma}_i^x$ , an  $\hat{\sigma}_i^z$ , or both operators, and 0 otherwise.)

Note that the string operators in Eq. (8) were conveniently defined as product of real operators, using  $\hat{\sigma}^x$  and  $\hat{\sigma}^z$ s, to avoid factors of  $i$  when making the connection with the cipher attacks. The effect of  $\hat{\sigma}^y$ s appears when  $\hat{\sigma}^x$  and  $\hat{\sigma}^z$  operators overlap in the string  $\hat{S}_\alpha$ ; we count the number of such overlaps by  $n_y(\alpha) \equiv \alpha^x \cdot \alpha^z$ . These strings are not self-conjugate and satisfy

$$\hat{S}_\alpha^\dagger = (-1)^{\alpha^x \cdot \alpha^z} \hat{S}_\alpha, \tag{17}$$

which in turn leads to the following symmetry relation, preserved throughout the evolution:

$$A_{\beta\alpha}^*(\tau) = (-1)^{\beta^x \cdot \beta^z} (-1)^{\alpha^x \cdot \alpha^z} A_{\beta\alpha}(\tau). \tag{18}$$

For permutations, the amplitudes are real, and this symmetry implies that  $A_{\beta\alpha}(\tau)$  is non-zero if and only if  $n_y(\alpha) = n_y(\beta) \bmod 2$ . In terms of the permutations  $P(x)$  on the bit strings  $x$ , the amplitudes take values in a discrete set, as can be seen from the explicit formula:

$$\begin{aligned}
A_{\beta\alpha}(\tau) &= \frac{1}{2^n} \sum_x \langle x | \hat{P}^\dagger \hat{S}_\beta \hat{P} \hat{S}_\alpha^\dagger | x \rangle = \frac{1}{2^n} \sum_x \langle x | \hat{P} \hat{S}_\alpha^\dagger \hat{P}^\dagger \hat{S}_\beta | x \rangle \\
&= \frac{1}{2^n} \sum_x (-1)^{\alpha^z \cdot P^{-1}(x)} \langle P^{-1}(x) \oplus \alpha^x | P^{-1}(x \oplus \beta^x) \rangle (-1)^{\beta^z \cdot x} \\
&= \frac{1}{2^n} \sum_x (-1)^{\beta^z \cdot x} (-1)^{\alpha^z \cdot P^{-1}(x)} \delta_{\beta^x, x \oplus P(P^{-1}(x) \oplus \alpha^x)}.
\end{aligned} \tag{19}$$

For orthogonal transformations,  $\hat{O}$ , the amplitudes  $A_{\beta\alpha}(\tau)$  are real but continuous, and Eq. (18) implies that  $A_{\beta\alpha}(\tau)$  is non-zero if and only if  $n_y(\alpha) = n_y(\beta) \bmod 2$ , just as for permutations. For unitary transformations,  $\hat{U}$ , the amplitudes are also continuous and Eq. (18) implies two cases according to the relative parity of  $n_y(\alpha)$  and  $n_y(\beta)$ : (a) for  $n_y(\alpha) = n_y(\beta) \bmod 2$ , the amplitudes  $A_{\beta\alpha}(\tau)$  are real; and (b)  $n_y(\alpha) \neq n_y(\beta) \bmod 2$ , the amplitudes  $A_{\beta\alpha}(\tau)$  are purely imaginary.

We note that our discussion also applies for backpropagation via the inverse operators (e.g., the inverse permutation  $P^{-1}$ ) by exchanging  $\hat{P}$  and  $\hat{P}^\dagger$  through a “time-

reversal” transformation:

$$\begin{aligned}
A_{\alpha\beta}(-\tau) &\equiv \langle \alpha | \hat{U}_{P^{-1}} | \beta \rangle \\
&= \frac{1}{2^n} \text{tr} \left( \hat{P} \hat{S}_\alpha \hat{P}^\dagger \hat{S}_\beta^\dagger \right) \\
&= A_{\beta\alpha}^*(\tau).
\end{aligned} \tag{20}$$

## A. Delocalization in string space

Given the operator-to-state correspondence defined above, the main results of the paper will follow from the behavior of the string amplitudes  $A_{\beta\alpha}(\tau)$  as function of  $\tau$ . These wave function amplitudes will allow us to quantify (a) the delocalization in string space in analogy with measures of (de)localization in quantum systems, and (b) the time,  $\tau_{\text{scramble}}$ , needed for the amplitudes to approach

those of a maximally scrambled state. In particular, this random state is the equilibrium state with maximum entropy and vanishing OTOCs. The connection between attacks and OTOCs implies that the random classical circuit leads to a secure cipher after time  $\tau_{\text{scramble}}$ .

For a fixed initial string state  $\alpha$ , the amplitudes  $A_{\beta\alpha}$  represent a wave function in a  $d = 4^n$  dimensional Hilbert space. Delocalization in this space can be quantified via the generalized inverse participation ratios and their associated entropies that are defined, respectively, by

$$\mathcal{P}_q = \sum_{\beta} |A_{\beta\alpha}(\tau)|^{2q}, \quad (21)$$

and

$$S_q = \frac{1}{1-q} \ln \mathcal{P}_q. \quad (22)$$

These provide concrete and intuitive measures of information scrambling, reflected in the proliferation of strings and delocalization in string space. In particular:  $\mathcal{P}_{q \rightarrow 0+}$  measures the number of non-zero amplitudes  $A_{\beta\alpha}$ , thus counting the number of strings,

$$\mathcal{N}_s = \mathcal{P}_{q \rightarrow 0+}; \quad (23)$$

$S_{q \rightarrow 1}$  gives the information entropy,

$$S = - \sum_{\beta} |A_{\beta\alpha}(\tau)|^2 \ln (|A_{\beta\alpha}(\tau)|^2); \quad (24)$$

and

$$\mathcal{P}_2 = \sum_{\beta} |A_{\beta\alpha}(\tau)|^4 \quad (25)$$

is the inverse participation ratio, familiar from the theory of localization in quantum systems [13].

## V. EQUILIBRIUM

Before we focus on the dynamics of delocalization in string space and the approach to equilibrium, we discuss the asymptotic equilibrium state. At equilibrium, the string wave functions  $A_{\beta\alpha}$  become independently distributed over string space, i.e., over different initial and final states  $\alpha$  and  $\beta$ . The independent distributions are however constrained by the normalization condition, Eq. (14), the parity condition, Eq. (18), as well as the symmetry class of the underlying transformation defining the computation. Below we derive the explicit probability distributions for the amplitudes  $A_{\beta\alpha}$  for the three symmetry classes associated with permutations, orthogonal, and unitary transformations.

### A. Random permutations

We start by considering the equilibrium statistical properties of the string amplitudes  $A_{\beta\alpha}$  for truly random permutations, with no reference as to how they are

built. In particular, we compute the probability distribution for the string amplitudes  $A_{\beta\alpha}$ , from which we obtain the generalized inverse participation ratios and entropies characterizing the equilibrium state.

The form of the probability distributions of the  $A_{\beta\alpha}$  amplitudes can be obtained explicitly in the large- $d$  regime as follows. Starting from Eq. (19), notice that the values of  $\beta^x$  that collect non-zero contributions from the summation over binary states  $x$  must satisfy

$$\beta^x = x \oplus \tilde{P}(x), \quad (26)$$

where

$$\tilde{P}(x) \equiv P(P^{-1}(x) \oplus \alpha^x). \quad (27)$$

For any permutation  $P$ , the associated permutation  $\tilde{P}$  is an involution, i.e.,  $\tilde{P}^2 = \mathbb{I}$ , for any  $\alpha^x$ . Now notice that the pair of state values  $x$  and  $\tilde{P}(x)$  contribute to the same  $\beta^x$  “box”, since  $x \oplus \tilde{P}(x) = \tilde{P}(x) \oplus \tilde{P}(\tilde{P}(x)) = \tilde{P}(x) \oplus x$ . We thus partition the set of  $N = 2^n$  values of  $x$  into  $N/2$  pairs  $(x_1, x_2), \dots, (x_{N-1}, x_N)$ , where  $x_{2j} = \tilde{P}(x_{2j-1})$ ,  $j = 1, \dots, N/2$ . For a random  $P$ , the number of pairs that fall into a given  $\beta^x$  box (due to  $x_{2j-1} \oplus x_{2j} = \beta^x$ ) should be Poisson distributed, i.e., the probability that  $m$  pairs fall into box  $\beta^x$  is

$$p_m = e^{-1/2} \frac{1}{m!} \frac{1}{2^m}, \quad (28)$$

where the Poisson parameter is  $1/2$  (since there are  $N/2$  pairs for  $N$  boxes).

Next, let us consider the phases, i.e., signs of contributions to Eq. (19). The phases coming from the two entries in a pair interfere either constructively if  $\beta^x \cdot \beta^z = \alpha^x \cdot \alpha^z \pmod{2}$ , or destructively if  $\beta^x \cdot \beta^z \neq \alpha^x \cdot \alpha^z \pmod{2}$ . The two cases can be considered together by defining  $\eta \equiv \beta^x \cdot \beta^z + \alpha^x \cdot \alpha^z \pmod{2}$ . More precisely, by using the identities  $P^{-1}(\tilde{P}(x)) = P^{-1}(x) \oplus \alpha^x$  [see Eq. (27)] and  $\tilde{P}(x) \oplus \beta^x = x$  [see Eq. (26)], we can relate the phases associated with the two partners,  $\tilde{P}(x)$  and  $x$ , in a pair as follows:

$$\begin{aligned} & (-1)^{\beta^z \cdot \tilde{P}(x)} (-1)^{\alpha^z \cdot P^{-1}(\tilde{P}(x))} \\ &= (-1)^{\beta^z \cdot \tilde{P}(x)} (-1)^{\alpha^z \cdot P^{-1}(x)} (-1)^{\alpha^z \cdot \alpha^x} \\ &= (-1)^{\beta^z \cdot \tilde{P}(x)} (-1)^{\alpha^z \cdot P^{-1}(x)} (-1)^{\beta^z \cdot \beta^x} (-1)^\eta \\ &= (-1)^{\beta^z \cdot [\tilde{P}(x) \oplus \beta^x]} (-1)^{\alpha^z \cdot P^{-1}(x)} (-1)^\eta \\ &= (-1)^{\beta^z \cdot x} (-1)^{\alpha^z \cdot P^{-1}(x)} (-1)^\eta, \end{aligned} \quad (29)$$

and thus, as claimed above, the two contributions come either with the same sign if  $\eta$  is even, or with opposite signs if  $\eta$  is odd.

The interference described above implies that only half of the values of  $\beta^z$  result in a non-zero amplitude, which is computed as follows. Members of each pair will add  $\pm 1$  in phase, and thus contribute either  $+2$  or  $-2$  to the amplitude. Let  $m_{\pm}$  denote the number of pairs falling within a  $\beta^x$  box contributing  $\pm 2$ , respectively. The probability that the amplitude  $A = 2r/N$  is

$$\begin{aligned}
p(A = 2r/N) &= \sum_m e^{-1/2} \frac{1}{m!} \frac{1}{2^m} \sum_{m_+ + m_- = m} \frac{m!}{m_+! m_-!} \frac{1}{2^{m_+}} \frac{1}{2^{m_-}} \delta_{r, m_+ - m_-} \\
&= e^{-1/2} \sum_{m_+, m_-} \frac{1}{m_+!} \frac{1}{m_-!} \frac{1}{4^{m_+}} \frac{1}{4^{m_-}} \delta_{r, m_+ - m_-} \\
&= e^{-1/2} \sum_k \frac{1}{(|r| + k)!} \frac{1}{k!} \left(\frac{1}{4}\right)^{|r| + 2k} \\
&= \frac{1}{\sqrt{e}} I_{|r|}(1/2), \tag{30}
\end{aligned}$$

where  $I_{\nu}(z)$  is the modified Bessel function.

To compute the moments, it is useful to introduce the generating function

$$\begin{aligned}
\tilde{p}(w) &= \sum_{r=-\infty}^{\infty} p(A = 2r/N) e^{iwr} \\
&= e^{-1/2} \sum_{m_+, m_-} \frac{1}{m_+!} \frac{1}{m_-!} \frac{1}{4^{m_+}} \frac{1}{4^{m_-}} e^{iw(m_+ - m_-)} \\
&= e^{-\frac{1}{2}} e^{\frac{1}{2} \cos w}. \tag{31}
\end{aligned}$$

The corresponding (averaged) generalized participation ratios are given by

$$\overline{P}_q = d^{1-q} 2^{2q-1} \frac{1}{\sqrt{e}} \left( -i \frac{\partial}{\partial w} \right)^{2q} e^{\frac{1}{2} \cos w} \Big|_{w=0}. \tag{32}$$

The associated equilibrium entropies display an extensive (volume) contribution and a correction,  $\Delta S_q^{\text{eq}}$ , of order 1:

$$S_q^{\text{eq}} = n \ln 4 - \Delta S_q^{\text{eq}}, \tag{33}$$

where

$$\Delta S_q^{\text{eq}} = \frac{1}{q-1} \ln \left[ \frac{1}{2\sqrt{e}} \left( -2i \frac{\partial}{\partial w} \right)^{2q} e^{\frac{1}{2} \cos w} \Big|_{w=0} \right]. \tag{34}$$

(We note that in calculating the entropies we used annealed averages, since in the regime of delocalized string wave functions the quenched and annealed averages should coincide up to exponentially small corrections.)

For integer values, the  $\Delta S_q^{\text{eq}}$  corrections can be read off from Eq. (34): for example  $\Delta S_2^{\text{eq}} = \ln 10$ ,  $\Delta S_3^{\text{eq}} = \frac{1}{2} \ln 196 = \ln 14$ , and  $\Delta S_4^{\text{eq}} = \frac{1}{3} \ln 6280$ . The value  $\Delta S_1^{\text{eq}} = 1.9618961$  is obtained numerically from the probabilities in Eq. (30). These residual entropies are used in the next sub-section to diagnose the quality of a Feistel cipher.

## B. Application to Feistel ciphers

A Feistel cipher, also referred to as a Luby-Rackoff cipher [1, 2], builds a pseudorandom permutation by using pseudorandom functions. The construction of the cipher proceeds by first separating  $n$  bits ( $n$  even) into left ( $L$ ) and right ( $R$ ) registers with  $n/2$  bits each. Denoting the input to the cipher by the pair  $(L_0, R_0)$ , one then iterates through rounds  $k = 1, \dots, r$ , according to:

$$\begin{aligned}
L_k &= R_{k-1} \\
R_k &= L_{k-1} \oplus f_k(R_{k-1}), \tag{35}
\end{aligned}$$

where  $f_k$ ,  $k = 1, \dots, r$ , are different pseudorandom functions with  $n/2$ -bit inputs and outputs. The iterations in Eq. (35) define a permutation  $P$  such that  $(L_r, R_r) = P(L_0, R_0)$ . The inverse permutation,  $(L_0, R_0) = P^{-1}(L_r, R_r)$ , is obtained by starting with  $(L_r, R_r)$  and working backwards, for  $k = r, \dots, 1$ , using the recursion

$$\begin{aligned}
R_{k-1} &= L_k \\
L_{k-1} &= R_k \oplus f_k(R_{k-1}). \tag{36}
\end{aligned}$$

Luby and Rackoff [2] proved that a 3-round (4-round) cipher is indistinguishable from a random permutation when interrogated with a polynomial number of one-sided or plaintext queries (two-sided or plaintext/ciphertext queries). [An example of a plaintext/ciphertext attack on a 3-round Feistel cipher was represented as an OTOC in Eq. (7).]

Below we apply our criterium for a secure cipher based on the saturation of the entropies to the Luby-Rackoff cipher. We compute the entropies defined in Eq. (22) using the string amplitudes  $A_{\beta\alpha}$  in Eq. (19), calculated by using the permutations  $P, P^{-1}$  of the Feistel cipher for an initial string  $\alpha$  that corresponds to a  $\hat{\sigma}^x$  operator (or NOT gate) on a bit on the  $L$  register of the cipher. As shown in Fig. 1(a), we find that the entropy  $S_1$  marches to its asymptotic equilibrium value  $S_1^{\text{eq}}$  [see Eq. (33)] as



the number of rounds increases. Figure 1(b) displays the average (over different realizations of ciphers) residual entropy  $S_1^{\text{eq}} - \bar{S}_1$ , and shows that the extensive contribution is saturated for 3 or more rounds, as reflected in the crossing of the curves for different block sizes at exactly 3 rounds. However, the saturation of the remaining order 1 contribution to the asymptotic equilibrium value,

$\Delta S_1^{\text{eq}} = 1.9618961$ , computed in the previous subsection requires at least 4 rounds. The same saturation behavior is illustrated in Table I for other entropies ( $q \neq 1$ ). It is important to note that at 4 (or more) rounds  $\Delta S_1^{\text{eq}} - \Delta \bar{S}_1$  vanishes exponentially in the number of bits,  $n$ , as seen in the inset to Fig. 1(b).

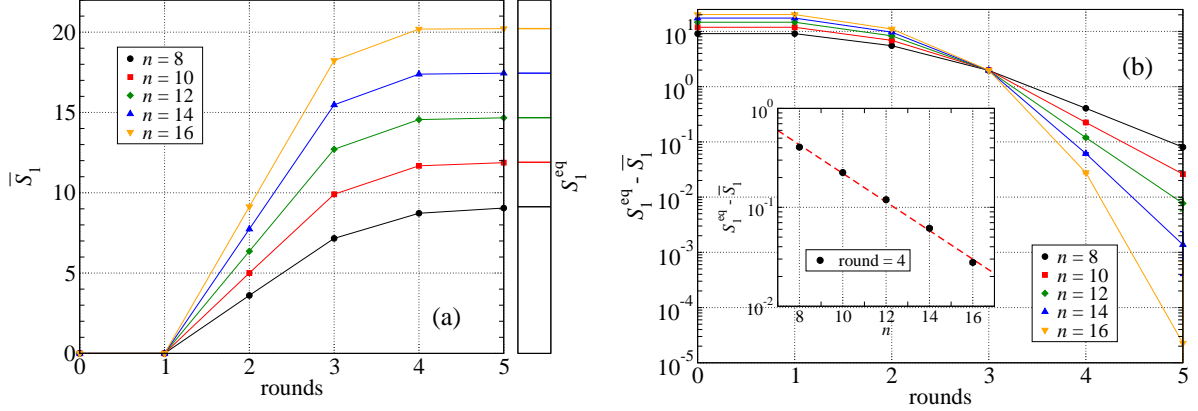


FIG. 1. (a) Average entropy,  $\bar{S}_1$ , over different realizations of Feistel ciphers, as a function of the number of rounds, for different block sizes,  $n$ . The initial string contains a single  $\hat{\sigma}^x$  on the  $L$  register ( $\alpha^z = 0$  and  $\alpha^x = 2^{n/2-1}$ ). The number of Feistel ciphers used in the averaging range from 500 ( $n = 8$ ) to 100 ( $n = 16$ ). Solid lines on the left panel are guides to the eye. The solid lines on the right panel show the equilibrium entropy values. (b) The deviation of entropy in panel (a) from the equilibrium value  $S_1^{\text{eq}}$ . Notice that the deviations increase (decrease) with  $n$  below (above) 3 rounds, whereas the deviation is independent of  $n$  after exactly 3 rounds. The inset in (b) shows the decrease in the deviation from the equilibrium entropy after 4 rounds as a function of the number of bits. The dashed line corresponds to the fitted function  $S_1^{\text{eq}} - \bar{S}_1 = 6.2(9) e^{-0.33(1)n}$ , where numbers in parentheses indicate standard errors. Pseudorandom functions used to build an  $n$ -bit cipher,  $f_k$ ,  $k = 1, \dots, r$ , are obtained by  $r$   $n/2$  sequential calls to a pseudorandom bit function with equal probability between 0 and 1 outputs.

The analysis of the entropy saturation gives an intuitive interpretation of the Luby and Rackoff results. Without knowledge of any specific attack, the order 1 residual entropy of 3-round ciphers underscores the vulnerability to an attack that can uncover of the order of

1 bit of information. At the same time, the exponential decay (with  $n$ ) of the residual entropy of 4-round ciphers reflects the fact that such ciphers are secure against any polynomial attack.

	round 1	round 2	round 3	round 4	round 5	rand. perm. (numerical)
$S_1^{\text{eq}} - \bar{S}_1$	22.1807	11.08(1)	1.98(1)	0.028(1)	0.00002(67)	0.00016(49)
$S_2^{\text{eq}} - \bar{S}_2$	22.1807	11.07(1)	2.7(1)	0.053(4)	0.0005(8)	0.00036(64)
$S_3^{\text{eq}} - \bar{S}_3$	22.1807	11.05(2)	4.1(3)	0.124(14)	0.0013(13)	0.00064(87)

TABLE I. Average residual entropies computed after rounds of a 16-bit Feistel cipher. Initial states and values of  $\alpha^z$  and  $\alpha^x$  are the same as those used in Fig. 1. 100 circuits are used to compute the average. Numbers in parentheses indicate standard deviations. The right-most column shows the residual entropy values for 16-bit random permutations computed numerically (average over 100 permutations). The values of  $S_q^{\text{eq}} = 16 \ln 4 - \Delta S_q^{\text{eq}}$  for the  $q$  shown are computed from Eq. (33) with the corrections in Eq. (34), explicitly  $\Delta S_1^{\text{eq}} = 1.9618961$ ,  $\Delta S_2^{\text{eq}} = \ln 10$ , and  $\Delta S_3^{\text{eq}} = \ln 14$ .

### C. Orthogonal and Unitary transformations

The probability of the string amplitudes  $A_{\beta\alpha}$  are much easier to compute for orthogonal and unitary transformations, which unlike permutations are continuous.

For the orthogonal case, the amplitudes are real and the distribution is Gaussian, with the width determined by the normalization condition in Eq. (14). The symmetry condition in Eq. (18) restricts the set of string labels  $\alpha$  which lead to non-zero amplitudes to those satisfying the parity condition  $n_y(\alpha) = n_y(\beta) \bmod 2$ . This condition eliminates amplitudes on half of the string space, and thus the Gaussian distribution for the remaining  $d/2$  states has width  $\sqrt{2/d}$ :

$$p_O(A_{\beta\alpha}) = \sqrt{\frac{d}{4\pi}} e^{-\frac{d}{4} A_{\beta\alpha}^2}. \quad (37)$$

For the unitary case, the symmetry condition in Eq. (18) dictates that the amplitudes are real for  $n_y(\alpha) = n_y(\beta)$  even, and purely imaginary for  $n_y(\alpha) = n_y(\beta)$  odd. By contrast to the orthogonal case, the amplitudes are non-vanishing in all  $d$  states, and thus the width of the Gaussian distribution is  $\sqrt{1/d}$ :

$$p_U(A_{\beta\alpha}) = \sqrt{\frac{d}{2\pi}} e^{-\frac{d}{2} |A_{\beta\alpha}|^2}. \quad (38)$$

These probability distributions lead to the following order-1 corrections to the entropies:

$$\Delta S_q^O = \ln 4 + \frac{1}{q-1} \ln \frac{\Gamma(q + \frac{1}{2})}{\Gamma(\frac{3}{2})} \quad (39)$$

and

$$\Delta S_q^U = \ln 2 + \frac{1}{q-1} \ln \frac{\Gamma(q + \frac{1}{2})}{\Gamma(\frac{3}{2})}. \quad (40)$$

### D. Vanishing of OTOCs at equilibrium

For all three symmetry classes, the OTOCs vanish in the equilibrium state. For independently and identically distributed amplitudes  $A_{\beta\alpha}$ , the ensemble average of the expression in Eq. (16) factorizes into products of clusters of  $2p$   $A$ 's. In each of these clusters the states  $\gamma_i$  must be equal, and the cluster contributes a factor of  $\overline{A^{2p}}$ . In all of the three symmetry classes discussed above,  $\overline{A^{2p}} \sim d^{-p}$ . The number of independent  $\gamma$ 's to be summed is  $\sum_p n_p - 1$ , where  $n_p$  is the number of clusters of size  $2p$ , and the  $-1$  comes from the Kronecker  $\delta$ 's in Eq. (16), which reduce the number of independent  $\gamma$ 's by 1. It thus follows that the contribution to the OTOC from a given partition scales as  $d^{-1+\sum_p n_p - \sum_p n_p p}$ . It is then clear that the OTOCs are dominated by partitions with clusters of size 2 (or  $p = 1$ ), with all other partitions contributing higher powers of  $d^{-1}$ . For the case of size 2

clusters, the contribution of a partition vanishes as  $d^{-1}$ , the inverse of the size of the string Hilbert space. We note that the argument above did not take into account the phase factors coming from the traces over the products of string operators in Eq. (16); these factors can only further decrease the OTOCs. In closing this section, we stress that reaching equilibrium, or equivalently, independently and identically distributed amplitudes  $A_{\beta\alpha}$  that result in the vanishing of arbitrary order OTOCs, can only be attained through the use of a universal set of gates, as will become clear in the next section.

## VI. DYNAMICS AND APPROACH TO EQUILIBRIUM

For permutations, the dynamics of the string amplitudes is determined by the specific implementation of the  $P$ , for example, either through the rounds of a Feistel cipher or through the application of a universal set of classical gates. Here we focus on the evolution via a random classical circuit decomposed in terms of 3-bit gates in the symmetric group  $S_8$ , each of which leads to a transition amplitude in string space of the form

$$\begin{aligned} t_{\alpha'\alpha}^{(g)} &= \langle \alpha' | \hat{g} | \alpha \rangle \\ &= \frac{1}{2^n} \text{tr} \left( \hat{g}^\dagger \hat{S}_{\alpha'} \hat{g} \hat{S}_\alpha^\dagger \right), \end{aligned} \quad (41)$$

where the string states  $\alpha, \alpha'$  may differ only in a substring of size 3. The transition amplitude  $t_{\alpha'\alpha}^{(g)}$  implemented by a single gate  $g$  satisfies the same normalization conditions as the  $A_{\beta\alpha}$ , namely:  $\sum_\alpha |t_{\alpha'\alpha}^{(g)}|^2 = \sum_{\alpha'} |t_{\alpha'\alpha}^{(g)}|^2 = 1$ .

These matrix elements control the spreading of the string wave function in the  $d = 4^n$  dimensional space of strings, analogous to the spreading taking place in random quantum circuits that deploy random unitary or orthogonal 2-qubit gates that are drawn from elements of  $U(4)$  or  $O(4)$ , respectively. The essential feature that controls quantum diffusion and delocalization in string space is the connectivity of a given string state,  $\alpha$ , to multiple states,  $\alpha'$ , a feature which is common to all three gate-set symmetry classes mentioned above. Below we discuss these three classes of circuits – those using 3-bit gates in  $S_8$  or 2-qubit gates in  $U(4)$  or  $O(4)$  – on equal footing.

To quantify spreading, we will consider powers of the transition probabilities  $|t_{\alpha'\alpha}^{(g)}|^2$ ,

$$T_{\alpha'\alpha}^q = \frac{1}{|G|} \sum_{g \in G} |t_{\alpha'\alpha}^{(g)}|^{2q}, \quad (42)$$

averaged over the group  $G$  for the given gate set, and the sum over these quantities over all final states  $\alpha'$ ,

$$V_\alpha^q = \sum_{\alpha'} T_{\alpha'\alpha}^q, \quad (43)$$

which are measures of the connectivity of the state  $\alpha$ , averaged over the gates. Notice that  $V_\alpha^{q=1} = 1$  follows from the normalization condition  $\sum_{\alpha'} |t_{\alpha'\alpha}^{(g)}|^2 = 1$ , and thus in diagnosing string spreading we must consider  $V_\alpha^q$  for  $q \neq 1$ . Since for a fixed initial state  $\alpha$  the  $|t_{\alpha'\alpha}^{(g)}|^2$  are probabilities, it is also useful to introduce an associated entropy

$$s_\alpha = -\frac{d}{dq} V_\alpha^q \Big|_{q \rightarrow 1} = -\sum_{\alpha'} \frac{1}{|G|} \sum_{g \in G} |t_{\alpha'\alpha}^{(g)}|^2 \ln |t_{\alpha'\alpha}^{(g)}|^2. \quad (44)$$

As the simplest example, consider 2-bit gates in  $S_4$  or 2-qubit Clifford gates [29, 30], in which case  $|t_{\alpha'\alpha}^{(g)}|^2$  is a permutation matrix, i.e., it connects single initial

and final states, resulting in  $V_\alpha^q = 1$  for all  $q$ 's, and the vanishing of the entropy  $s_\alpha$ . By contrast, for 3-bit gates in  $S_8$  and 2-qubit unitary and orthogonal gates,  $V_\alpha^q \neq 1$  for  $q \neq 1$ , and  $s_\alpha > 0$ . Table II displays the values of  $V_\alpha^{q \rightarrow 0}$ , which measures the average connectivity of a state  $\alpha$ , and the entropy  $s_\alpha$ . These results follow from the detailed structure of the matrix  $T_{\alpha'\alpha}^q$  for 3-bit gates in  $S_8$ , and 2-qubit gates in  $U(4)$  and  $O(4)$ , shown in Fig. 2. For all three sets of gates and in all non-trivial subspaces,  $V_\alpha^{q \rightarrow 0} > 1$  and  $s_\alpha > 0$ . It is then clear that string proliferation builds up exponentially through the application of a sufficiently large number of consecutive gates. It is this proliferation that evolves the entropies to their saturation values and leads to vanishing OTOCs in the asymptotic equilibrium state.

Measure	3-bit gates in $S_8$				2-qubit gates in $O(4)$			2-qubit gates in $U(4)$	
	Sector				Sector			Sector	
	identity	z-strings	odd parity	even parity	identity	odd parity	even parity	identity	other strings
$V_\alpha^{q \rightarrow 0}$	1	17/5	51/5	103/10	1	3	9	1	15
$s_\alpha$	0	1.11	2.03	2.08	0	0.67	1.34	0	1.90

TABLE II. Diagnostics for 3-bit permutation gates from  $S_8$ .

#### A. The OTOC application to the avalanche criterium: Mean Field Theory

We use the information above to analyze the simplest OTOC presented in Eq. (6) that quantifies the avalanche effect [26–28]. Using Eq. (16), with  $\hat{S}_\alpha = \hat{\sigma}_i^x$  and  $\hat{S}_\beta = \hat{\sigma}_j^z$ , we can write the OTOC in terms of the string space amplitudes (see Appendix B):

$$\begin{aligned} C_{\text{SAC}}^{ij} &= \sum_{\gamma | \hat{\sigma}_i^z \notin \hat{S}_\gamma} |A_{\gamma\beta}(-\tau)|^2 - \sum_{\gamma | \hat{\sigma}_i^z \in \hat{S}_\gamma} |A_{\gamma\beta}(-\tau)|^2 \\ &= p_{0|\beta} - p_{z|\beta}. \end{aligned} \quad (45)$$

This expression measures the difference of probabilities  $p_{0|\beta}$  and  $p_{z|\beta}$ , respectively, that the strings contain either an identity or a  $\hat{\sigma}^z$  operator at position  $i$ , given the initial string  $\beta$  that contains identities at all locations except for location  $j$ . The OTOC will vanish once the string wave function is delocalized in string space, in which case the contributions from the two terms in Eq. (45) balance each other to the desired accuracy. (Below we shall define the string density  $\rho = p_z$ , in terms of which  $C_{\text{SAC}}^{ij} = 2\rho - 1$ .)

Notice that the initial state in Eq. (6) is a weight 1  $z$ -string, and as is clear from the structure of the transition matrix shown in Fig. 2, the  $z$ -nature of the string is preserved throughout the evolution. We proceed with

an analysis that parallels that of Brown and Farzi in Ref. [17, 18] in the study of random unitary circuits, which further underscores the formal connection between classical and quantum circuits, when viewed in string space. The OTOC in Eq. (45) depends only on the string probabilities (squares of the amplitudes) which when averaged over circuits, evolve according to a Markov process defined in terms of the averaged transition probabilities in Eq. (42) with  $q = 1$ . We remark that in the unitary case, the Markov chain involves  $16 \times 16$  average transition matrices with non-trivial  $15 \times 15$  blocks [see Fig. 2(c)], and acts on general strings involving all 4 Pauli operators. In considering Eq. (45), the Markov chain involves  $8 \times 8$  matrices with non-trivial  $7 \times 7$  blocks [see the first two blocks in Fig. 2(a)], which act on amplitudes of strings containing only  $\hat{\sigma}^z$  and the identity. In spite of the differences in the details of the block structures, the splitting of single string states into superpositions is common to all these problems; as a result, we expect that the scaling behavior with system size proved in Refs. [17, 18, 20] also applies to the circuits with gates in  $S_8$ , and thus the minimum size circuit required for the OTOC Eq. (45) to vanish to superpolynomial precision is no larger than  $\mathcal{O}(n \ln^2 n)$ .

Below we argue that a shorter circuit with  $\mathcal{O}(n \ln n)$  gates should suffice. In the context of unitary cir-

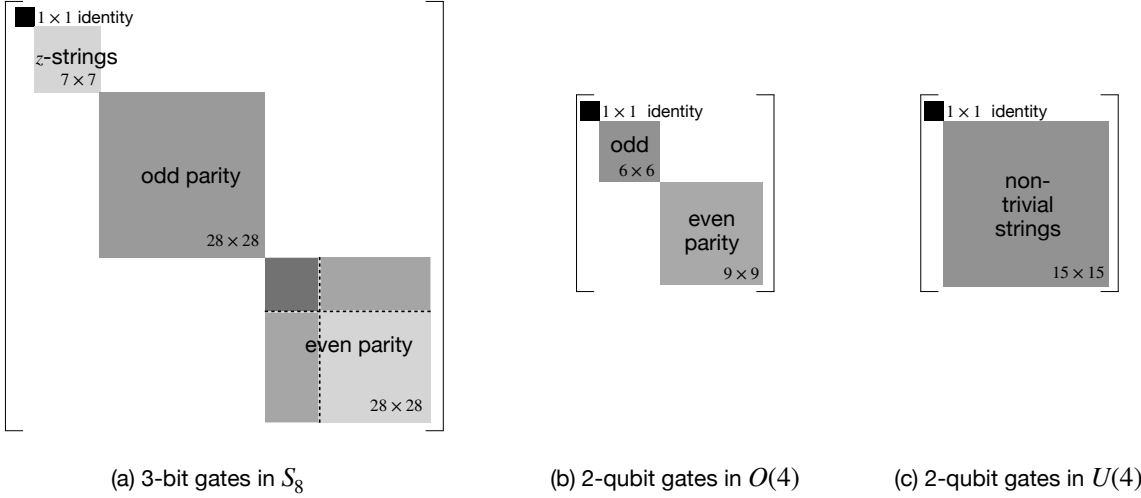


FIG. 2. Block form for the matrices  $T_{\alpha'}^q$  in Eq. (42) for the three symmetry classes. (a) For 3-bit permutation gates, the  $4^3 \times 4^3$  matrix  $T^q$  breaks up into 4 blocks of sizes  $1 \times 1$ ,  $7 \times 7$ ,  $28 \times 28$ , and  $28 \times 28$ , reflecting the symmetries of the string space transition amplitudes. The  $1 \times 1$  block represents the transition between identity strings – tensor products of Pauli identity operators – that are invariant under evolution. The  $7 \times 7$  block connects only  $z$ -string states, i.e., those with  $\alpha_x = 0$ , which form an invariant subspace. The remaining two  $28 \times 28$  blocks correspond to transitions within subspaces with even or odd number  $n_y(\alpha)$  of  $\hat{\sigma}^y$  Pauli matrices or, equivalently, the number of overlapping  $\hat{\sigma}^x$  and  $\hat{\sigma}^z$  Pauli matrices on the substring. Recall from the discussion in connection with Eq. (18) that the parity of  $n_y(\alpha)$  is a conserved quantity. The matrix elements of  $T^q$  within each of the  $1 \times 1$ ,  $7 \times 7$ , and odd parity  $28 \times 28$  blocks are equal. The even parity  $28 \times 28$  block involves four sub-blocks: a diagonal  $7 \times 7$  block describing transitions between  $x$ -strings ( $\alpha_z = 0$ ); another diagonal  $21 \times 21$  block of transitions between the remaining odd parity state; and two off-diagonal,  $7 \times 21$  and  $21 \times 7$  rectangular blocks connecting these two subspaces. Within each of these sub-blocks, the matrix elements are the same. (b) For 2-qubit gates in  $O(4)$ , the  $4^2 \times 4^2$  matrix  $T^q$  breaks up into the trivial  $1 \times 1$  block (connecting the identity strings), a  $6 \times 6$  odd subsector, and a  $9 \times 9$  even subsector. The matrix elements are all equal within each block. (c) For the 2-qubit gates in  $U(4)$ ,  $T^q$  breaks into the identity block and a  $15 \times 15$  block, with all equal matrix elements, connecting all other states.

culits, this scaling form was alluded to by both Oliveira, Dahlsten, and Plenio [15] and Harrow and Mehraban [20]. Their difficulty in proving this stronger result is a subtle issue associated to rare events that arise in short circuits due to bits that are either untouched by gates or unaffected by the action of gates.

In order to gain a better understanding of both the  $\mathcal{O}(n \ln n)$  scaling and the origin of the rare events that force the weaker bound  $\mathcal{O}(n \ln^2 n)$  in Refs. [17, 18, 20], we start with a naive mean-field analysis of circuits with long-range random gates. We proceed by evolving the string amplitudes with the application of a single gate  $g$ :

$$A_{\beta\alpha}^2(\tau + 1) = \sum_{\gamma_1, \gamma_2} t_{\beta\gamma_1}^{(g)} t_{\beta\gamma_2}^{(g)} A_{\gamma_1\alpha}(\tau) A_{\gamma_2\alpha}(\tau), \quad (46)$$

which upon averaging over circuits leads to

$$\overline{A_{\beta\alpha}^2(\tau + 1)} = \sum_{\gamma} T_{\beta\gamma}^1 \overline{A_{\gamma\alpha}^2(\tau)}, \quad (47)$$

with  $T_{\beta\gamma}^1$  defined in Eq. (42).  $T_{\beta\gamma}^1$  acts non-trivially only on the 3-site substrings; summing over the indices of the untouched sites allows us to rewrite Eq. (47) in terms of

the 8 marginal probabilities  $p_{k|\alpha}$ ,  $k = 000, \dots, zzz$ , in the space of 3-site substrings:

$$p_{k|\alpha}(\tau + 1) = \sum_{k'} T_{k,k'}^1 p_{k'|\alpha}(\tau), \quad (48)$$

where  $T_{k,k'}^1$ , within the combined identity and  $z$ -string blocks, takes the form of an  $8 \times 8$  matrix

$$T^1 = \frac{1}{7} \begin{pmatrix} 7 & 0 & 0 & 0 & 0 & 0 & 0 & 0 \\ 0 & 1 & 1 & 1 & 1 & 1 & 1 & 1 \\ 0 & 1 & 1 & 1 & 1 & 1 & 1 & 1 \\ 0 & 1 & 1 & 1 & 1 & 1 & 1 & 1 \\ 0 & 1 & 1 & 1 & 1 & 1 & 1 & 1 \\ 0 & 1 & 1 & 1 & 1 & 1 & 1 & 1 \\ 0 & 1 & 1 & 1 & 1 & 1 & 1 & 1 \\ 0 & 1 & 1 & 1 & 1 & 1 & 1 & 1 \end{pmatrix}. \quad (49)$$

For the purposes of our discussion, we will focus on the string density,  $\rho$ , of non-trivial Pauli operators as the weight  $w$  of a string divided by  $n$ . We can compute the change in weight after the application of a random (ar-

bitrary range) 3-bit gate using the probabilities above,

$$\begin{aligned} \delta w &= \sum_k w_k [p_{k|\alpha}(\tau+1) - p_{k|\alpha}(\tau)] \\ &= \sum_{k,k'} (w_k - w_{k'}) T_{k,k'}^1 p_{k'|\alpha}(\tau), \end{aligned} \quad (50)$$

where  $w_k$  is the weight of the 3-site substring, and we used that  $\sum_k T_{k,k'}^1 = 1$ . The mean-field approximation of the exact equation Eq. (50) consists of writing the marginal probabilities of a substring configuration in terms of the density  $\rho$  itself. Explicitly, we substitute the marginal probability for an identity string  $p_{000} = (1-\rho)^3$ , for the 3- $\hat{\sigma}^z$  substring  $p_{zzz} = \rho^3$ , and similarly for the other 6 possibilities. Using this factorization of the marginals, we can use Eq. (50) and account for the transitions that decrease, preserve, or increase the weight of the string, yielding the following evolution equation for the average density:

$$\begin{aligned} n \frac{d\rho}{d\tau} &= (1-\rho)^3 \times 0 \\ &\quad + 3\rho(1-\rho)^2 \left[ \frac{3}{7} \times 0 + \frac{3}{7} \times 1 + \frac{1}{7} \times 2 \right] \\ &\quad + 3\rho^2(1-\rho) \left[ \frac{3}{7} \times (-1) + \frac{3}{7} \times 0 + \frac{1}{7} \times 1 \right] \\ &\quad + \rho^3 \left[ \frac{3}{7} \times (-2) + \frac{3}{7} \times (-1) + \frac{1}{7} \times 0 \right] \\ &= \frac{12}{7} \rho \left( \frac{1}{2} - \rho \right) \left( \frac{5}{2} - \rho \right). \end{aligned} \quad (51)$$

Above we detailed the probabilities of the transitions within the  $7 \times 7$   $z$ -string block in Eq. (49) [see also Fig. 2(a)], and the values by which the weight changes. By integrating the equation we obtain

$$\begin{aligned} \tau &= n \frac{7}{12} \left[ \frac{4}{5} \ln \frac{\rho_f}{\rho_i} - \ln \frac{1/2 - \rho_f}{1/2 - \rho_i} + \frac{1}{5} \ln \frac{5/2 - \rho_f}{5/2 - \rho_i} \right] \\ &= \frac{7}{12} n \left[ \frac{4}{5} \ln n + \ln(1/\epsilon) \right] + \mathcal{O}(1). \end{aligned} \quad (52)$$

where we used an initial state with weight 1, i.e.,  $\rho_i = 1/n$ , and a final  $\rho_f$  equal to the asymptotic value of  $1/2$  minus a correction  $\epsilon$ .

Carrying out the same simple mean-field calculation for the random 2-qubit unitary gates gives

$$\begin{aligned} n \frac{d\rho}{d\tau} &= (1-\rho)^2 \times 0 \\ &\quad + 2\rho(1-\rho) \left[ \frac{6}{15} \times 0 + \frac{9}{15} \times 1 \right] \\ &\quad + \rho^2 \left[ \frac{6}{15} \times (-1) + \frac{9}{15} \times 0 \right] \\ &= \frac{8}{5} \rho \left( \frac{3}{4} - \rho \right), \end{aligned} \quad (53)$$

which leads to

$$\tau = \frac{5}{6} n [\ln n + \ln(1/\epsilon)] + \mathcal{O}(1). \quad (54)$$

This mean-field calculation captures the evolution of the *average* density and provides an estimate of the number of gates required to reach the asymptotic value to within fixed  $\epsilon$  precision. What the mean-field approach misses is the detailed shape of the probability distribution, which includes the finite probability that strings remain small as the computation progresses. This effect disappears for sufficiently long circuits, but can have observable consequences for short circuits. There are two circumstances under which issues may arise. The first is the case in which a bitline is not touched by any gate  $g$  in the circuit, or equivalently, a certain string location is not acted on by any dual gate  $\hat{g}$ . However, one trivially eliminates this issue by arranging the gates in layers that always touch every bitline or substring. For these circuits the number of gates  $n_g = \ell n/3$  for 3-bit permutation gates (or  $n_g = \ell n/2$  for 2-qubit unitary gates), where  $\ell$  is the number of layers (the circuit depth).

The trickier situation involves a non-zero probability  $p$  (independent of  $n$ ) that a string of weight 1 does not increase even when touched by a (dual) gate. [The stay-probabilities,  $3/7$  and  $6/15$  for case of permutations and unitaries, respectively, can be read from the second lines of the mean-field Eqs. (51) and (53).] After  $\ell$  layers this probability decreases to  $\sim p^\ell$ , corresponding to a polynomial decay in  $n$  for  $\ell \sim \ln n$ . By contrast, the decay becomes super-polynomial for a circuit with  $\ell \sim (\ln n)^{1+\delta}$ ,  $\delta > 0$ . It is the latter and not the former that is necessary in order to implement a classical cipher that is secure against polynomial attacks.

The mean-field treatment describes the motion of the center of a biased random walk, but misses the tails of the distribution at low weights for short walks, the origin of problems described above. Below we will use the freedom afforded us in the context of ciphers to design circuits which from the very start eliminate the tails due to low weight strings already for circuits of depth  $\ell \sim \ln n$ , i.e., circuits with  $\mathcal{O}(n \ln n)$  gates.

## B. Multi-stage ciphers: string inflation and proliferation

We proceed by identifying two distinct processes controlling the evolution of string wave function amplitudes: (a) the extension of the weight of the string; and (b) the proliferation of the number string states with non-zero amplitudes. The latter, but not the former, requires the action of non-linear gates. Here we propose a two-step cipher that separates these two processes. We first apply gates for which the stay-probability for weight 1 substrings vanishes, thereby completely eliminating the tails of the distribution for low weight strings. Once the average density reaches its asymptotic value ( $3/4$  for a

general initial string), we apply the full set of gates. It is through this device that we realize an optimal cipher with a circuit of size  $\mathcal{O}(n \ln n)$ .

### 1. Inflation

The search for the special set of gates that eliminates the stay-probability for weight 1 substrings is found as follows. We compute the entries  $t_{\alpha'\alpha}^{(g)}$  of the  $64 \times 64$  transition in Eq. (41) for each of the  $8!$  gates in  $S_8$ . We filter out all gates for which the  $9 \times 9$  submatrix connecting the 9-dimensional subspace of weight 1 strings is non-zero, thus retaining only gates for which weight 1 substrings grow into weight 2 or 3 substrings. There are 144 such “inflationary” gates, which are linear and inflate the weight of an initially small string into a *single* string of macroscopic weight (of order  $3n/4$ ). Appendix C lists these gates explicitly and also represents them in terms of equivalent circuits of CNOTs.

To gain further insight into the effect of the 144 inflationary gates, we note that, in bit space, this set of gates has the following property: for any input state, flipping

one input bit flips at least 2 output bits. It follows that, after  $\ell$  layers, flipping one of the  $n$  input bits of a circuit leads to a cascade of  $2^\ell$  flipped output bits, and thus  $\ell = \log_2(n/2)$  layers suffice to change half of the output bits. It should be noted that, for a random circuit, the probability that two flipped bits appear as input to the same 3-bit gate is  $(n-2)/\binom{n}{3} \sim 1/n^2$ , and therefore the probability that inflation fails to proceed over  $\ln n$  layers,  $p_{\text{fail}} \sim 1/n^{2 \ln n}$ , decays faster than any power law in  $n$ . Thus, by using the inflationary gates in a circuit with depth  $\ln n$ , we changed the decay of the probability for rare events associated with the lack of growth of small strings from polynomial to superpolynomial in  $n$ . The effect of the inflationary gates in a two-stage circuit is illustrated through a comparison to the behavior in a generic random circuit in Fig. 3, where we display the evolution with  $\ell$  of the probability,  $p_k(\ell)$ , of flipping  $k$  bits at the output when a single bit is flipped at the input. The comparison highlights two features of the two-stage circuit: (i) the faster evolution of the average number of bit-flips,  $\bar{k}(\ell)$ , to its saturation value; and (ii) the sharp drop of the stay-probability at  $k = 1$ ,  $p_1(\ell)$ , after the first layer.

### 2. Proliferation

Following the inflationary period, applying a universal set of gates leads to an explosion of the single heavy string into exponentially many. In order to speed up the scrambling, instead of deploying the full set of  $8!$  gates in  $S_8$ , we use the subset of non-linear gates that maximizes string proliferations at each step. This set is identified from the entries  $t_{\alpha'\alpha}^{(g)}$  for every gate  $g$  by selecting those for which the number of non-zero elements in each line or column is maximal. We find 10752 gates satisfying this criterium. For all these gates the squares of the non-zero elements take the same values within each of the blocks shown in Fig. 2. In each line or column there are: 4 equal values of  $1/4$  in the  $7 \times 7$   $z$ -block; and 16 equal values of  $1/16$  in both the  $28 \times 28$  even and odd blocks. This structure implies that each of these gates lead to string proliferation with each and every application. We established the universal property of this set of gates by determining that the order of the group generated by particular pairs of gates in this set is  $8!$ <sup>2</sup>

The proliferation of strings induced by this set of gates is very rapid since each of them in a  $n/3$ -gate layer splits strings into a superposition of multiple strings. We note that the exponential proliferation of strings, which already happens in one layer, is by itself not sufficient to

equilibrate the system. To reach the asymptotic probability distribution of the string amplitudes requires a minimum number of such layers. This minimum number of layers is determined by the accuracy to which one requires the vanishing of the OTOCs or the saturation of the entropies. For a good cipher, which cannot be distinguished from a random permutation with a polynomial number of queries, this accuracy must be superpolynomial.

Because the proliferation stage is initiated from a macroscopic string, after a few applications of non-linear gates one reaches a many-string state in which expectation values are homogeneous in position, i.e., they become independent of location along the string. As a result, all further evolution towards equilibrium should be an exponentially decaying function of time alone. Here time is measured by the number of layers of  $n/3$  gates that are applied in parallel, as discussed above. The decay of the OTOCs and the residual entropies with time (the number of layers) depend on the specific connectivity of the circuit. Figure 4 shows the decay (past the end of the inflationary period<sup>3</sup>) of the square of the OTOC associated with the avalanche test, for different types of circuit layouts: (a) arrangements of randomly chosen local gates on ordered brickwall lattices in 1-, 2-, and 3-dimensions; and (b) arrangements of  $n/3$  randomly chosen 3-bit non-local (long-range) gates that act only once

<sup>2</sup> For example, the two permutations 01243675 and 73051246 suffice to generate  $S_8$ .

<sup>3</sup> When linear gates such as the inflationary gates are employed on the first stage of a circuit, the OTOC remains equal to 1.

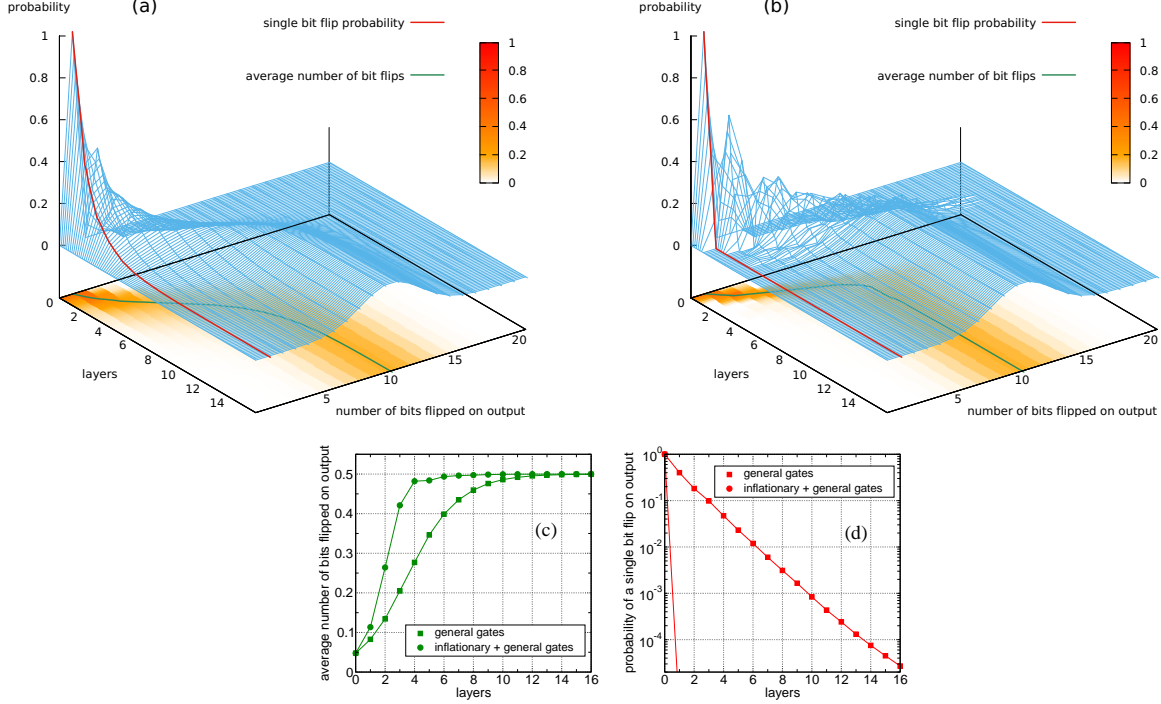


FIG. 3. Probability  $p_k(\ell)$  of flipping  $k$  bits at the output when a single bit is flipped at the input for a system of  $n = 21$  bits, after the deployment of  $\ell$  layers of gates. The probability distributions are computed numerically by averaging over all  $2^{21}$  input states, over which input bit is flipped, and over 256 circuits. (a) Gates are randomly drawn from the full set of  $8!$  3-bit gates in  $S_8$ . We note the gradual increase of  $\bar{k}(\ell)$  with  $\ell$  towards saturation at  $n/2$  (shown in green) and the (exponential) decay of the stay probability,  $p_1(\ell)$  (shown in red). (b) Gates are structured in a two-stage circuit with four layers of inflationary gates, followed by layers of the full set of gates in  $S_8$ . We note the faster saturation of  $\bar{k}(\ell)$  (green), and the abrupt drop of the stay probability,  $p_1(\ell)$  after one layer (red). (Recall the argument in the text explaining the superpolynomial suppression of the probability of stopping the inflation process.) (c) and (d), for  $\bar{k}(\ell)$  (green) and  $p_1(\ell)$  (red), respectively, juxtapose the results for the two sets of gates on the same plot. Solid lines are guides to the eye.

on every bit line – gate placements that we refer to as random long-range packed circuits. As can be seen from Fig. 4(a), the exponential decay of the OTOC as a function of the number of layers  $\ell$  becomes faster with increasing dimension. In the case of finite-dimension packing, i.e., case (a), the decay rate is independent of the system size (number of bits),  $n$ . By contrast, for the random long-range packed circuits in case (b) [see Fig. 4(b)], the decay rate accelerates as  $n$  increases.

For the  $D = 1$ -, 2-, and 3-dimensional systems in case (a), the OTOC decays as  $\sim e^{-\Gamma_D \ell}$  for large enough  $\ell$ , with  $\Gamma_D$  independent of  $n$ , and thus after  $\ell \sim \ln n$  layers the OTOC vanishes to polynomial precision in  $n$ . By contrast, for random long-range packed systems of same depth ( $\ell \sim \ln n$ ) the OTOC vanishes super-polynomially in  $n$  as  $\sim e^{-\Gamma(n)\ell} \sim n^{-\Gamma(n)}$ , with  $\Gamma(n)$  increasing with  $n$ . It is this  $n$  dependence of  $\Gamma(n)$  in the case of the long-range packed circuits that allows us to reach a cipher secure to polynomial number of queries with only  $\mathcal{O}(n \ln n)$  gates.

Below we argue that the data in Fig. 4(b) is consistent with  $\Gamma(n) \sim a \ln n + b$ . We note that the OTOC is in-

dependent of the number of bits for circuits with fewer than  $\log_3(n) - 1$  layers. Thus, defining  $k = \log_3(n)$  and  $\ell' = \ell - k + 1$ , we rescale the average square of the OTOC by its value at  $\ell' = 0$  and take its natural logarithm. Namely, we evaluate

$$Q_k(\ell') = \ln \left[ \frac{\frac{1}{n} \sum_j \overline{|C_{\text{SAC}}^{ij}|^2}(\ell')}{\frac{1}{n} \sum_j \overline{|C_{\text{SAC}}^{ij}|^2}(0)} \right]. \quad (55)$$

for various values of  $\ell'$  and  $k$ . Notice that  $Q_k(0) = 0$  for all  $k$ . This function increases linearly with  $\ell'$  thereon,  $Q_k(\ell' \rightarrow 0) = \alpha_k \ell'$ , and then saturates to a constant for large  $\ell'$ ,  $Q_k(\ell' \gg 1)$ , whose value depends on  $k$  and on the number of states used to sample the OTOC. The coefficient  $\alpha_k$  captures the dependence of the decay rate of the OTOC on  $k$ , which is extracted numerically and shown in Fig. 5. Notice that this coefficient increases approximately linearly with  $k$ , providing numerical evidence that  $Q_k \sim k\ell$ , or equivalently, that the OTOC decay rate is indeed faster than linear (with  $n$ ) by a factor proportional to  $k \sim \ln n$ .

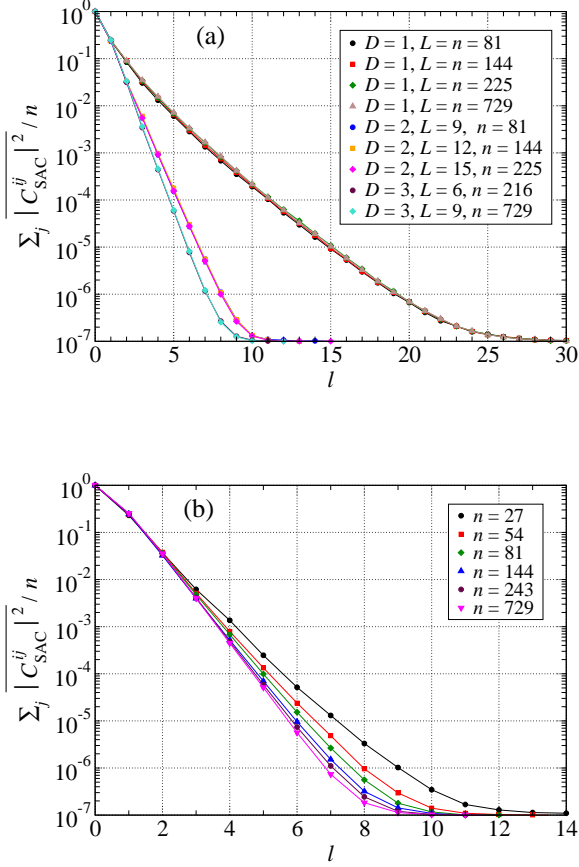


FIG. 4. Decay of the square of the OTOC as a function of the number of layers,  $\ell$ , past the end of the inflationary period, for different circuits of 3-bit random reversible gates: (a)  $D$ -dimensional brickwall arrangements (local) for  $D = 1, 2$  and 3 systems of linear size  $L$  and  $n = L^D$  bits; and (b) long-range packed circuits acting on  $n$  bits with a random gate arrangement. The OTOC is evaluated over  $M = 10^7$  random input states rather than all  $2^n$  configurations, hence the saturation of the decay at  $1/M$  upon squaring the OTOC. The squared OTOC is averaged over both  $j$  (output) bits and circuit realizations, with fixed flipped bit  $i = 0$  in all cases. Gates are drawn with uniform probability over the set of 10752 universal gates that maximize string proliferation, as discussed in the text. 16 to 64 circuit realizations are used for each case (statistical error bars are smaller than the data symbols and thus not visible). Solid lines are guides to the eye.

Finally, as we show in Fig. 6, in the proliferation stage, the entropy also decays exponentially in  $\ell$ . (We note that, starting with a single string, the entropy remains zero in the inflationary period, since linear gates conserve the number of strings.) The decay with  $\ell$  is clearly more rapid for the random long-range packed circuit of 3-bit universal gates than for the 1-dimensional circuit layout. Because the entropy is more costly to compute than the OTOCs, we are limited to small system sizes and, as a

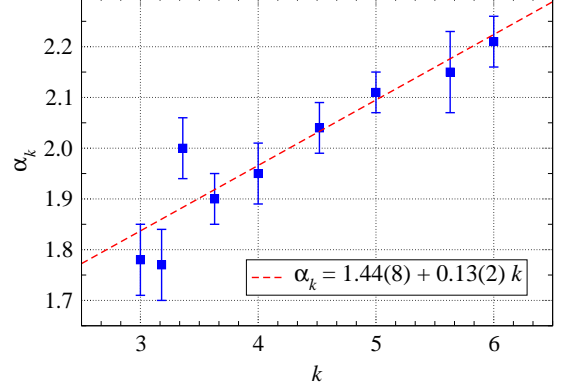


FIG. 5. Fitting to the data from Fig. 4(b) to obtain the OTOC decay rate coefficient (see text for explanation). Blue squares correspond to  $n = 27, 33, 42, 54, 81, 144, 243, 486$ , and 729. The dashed line indicates a linear fit to the data points, resulting in  $\alpha_k = 1.44(8) + 0.13(2)k$ .

result, we did not carry out a systematic analysis of the decay rates with  $n$ . An exponential decay with  $\ell$ , without an  $n$  dependence, implies that a circuit with  $(\ln n)^{1+\delta}$  layers or  $\mathcal{O}(n(\ln n)^{1+\delta})$  gates are needed to build a cipher secure to polynomial attacks, where  $\delta > 0$ . We conjecture that, as in the case of the SAC OTOC, the rate of decay of the residual entropy also increases with  $n$ , so that  $\mathcal{O}(n \ln n)$  gates suffice to attain superpolynomial security. We leave for future work the development of efficient sampling algorithms that would enable us to study the  $n$  dependence of the decay rates of the residual entropy.

## VII. CONCLUSIONS AND OPEN DIRECTIONS

In this paper we presented a framework for analysis and design of classical ciphers based on a close conceptual connection to the problem of scrambling of quantum states. The close parallels to quantum problems emerges naturally when we translate the actions of measuring or flipping bits describing cipher attacks to Pauli string operators. It is in string space that quantum mechanical-like concepts, such as superposition of states and operator spreading, become manifest. Here we studied the evolution of a classical computation in string space and connected measures of cipher security, such as resistance to plaintext and ciphertext attacks, to the vanishing of out-of-time-order correlators (OTOCs), which in quantum systems characterizes the appearance of chaos. Starting from any initial string state, in both classical and quantum random circuits, scrambling and chaos follow from the delocalization of amplitudes across the exponentially large Hilbert space of string states. We quantified this delocalization in string space in terms of participation ratios



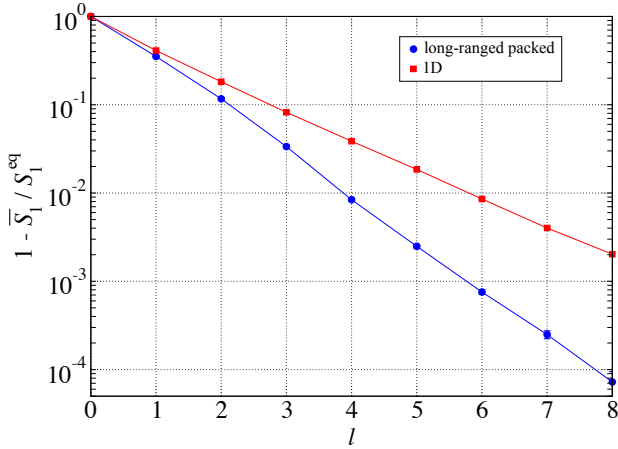


FIG. 6. Evolution of the rescaled average entropy with the number of layers,  $\ell$ , for a 1-dimensional (brickwall arrangement) circuit, and a for long-range packed circuit with random gate arrangement, both employing random 3-bit universal gates and acting on  $n = 15$  bits. The initial string state correspond to  $\alpha^z = 0$  and a fixed but random value for  $\alpha^x$ . 256 realizations of each type of circuit are used to compute the averages. Statistical error bars are smaller than the size of the data point symbols for most points and thus not always visible. Solid lines are guides to the eye.

and associated entropies. We argued that, in order for a cipher to be indistinguishable from a random permutation to polynomial accuracy, the OTOCs and residual entropies must vanish superpolynomially in the number of bits. An important conclusion of this paper is that this is achievable via random long-range packed circuits built out of layers of  $n/3$  non-overlapping 3-bit gates in  $S_8$ , with as few as  $\mathcal{O}(n \ln n)$  gates.

In order to reach this result we had to circumvent the effect of rare events and the associated tails in the distribution of string weights that is connected with the slow growth of initially small strings. The same problem appears in the analysis of scrambling by random quantum circuits, in which case overcoming these tails requires larger circuits. In particular, Brown and Fawzi [17, 18] prove scrambling and decoupling for circuits with  $\mathcal{O}(n \ln^2 n)$  gates, and Harrow and Mehraban [20] prove that circuits laid down in  $D \sim \ln n$  dimensional lattices would scramble with  $\mathcal{O}(n \ln n \ln \ln n)$  gates. (Ref. [20] also conjectures that one should be able to achieve scrambling with  $\mathcal{O}(n \ln n)$  gates, as we argued here.) The insight that allows us to establish our result for the shorter circuit is to separate two distinct processes controlling the evolution of string wave function amplitudes, which we apply sequentially. The first is the extension of small weight strings in the initial state to strings of macroscopic weight (of order  $3n/4$ ), a process we implement via a set of 144 special linear gates (out of the  $8!$  gates in  $S_8$ ). These “inflationary” gates have the property that the stay-probability for weight 1 substrings vanishes, ensuring that strings gain weight at a sufficiently fast rate that the tails decay superpolynomi-

ally with  $n$  already for a circuit with  $\mathcal{O}(n \ln n)$  gates. The second process involves applying all gates to the heavy string emerging from the inflationary period. During this string “proliferation” stage, the application of a typical non-linear gate splits a string state into a superposition of multiple heavy string states, rapidly leading to an exponential number of non-zero string amplitudes. As discussed in the text, it is this proliferation in string space that leads to the maximum entropies defined from the string state probabilities and to the vanishing of OTOCs characterizing scrambling.

We end with comments on three issues that may inspire future work. First, the two-stage process that we employed in the context of the classical cipher can also be implemented in a packed random long-range quantum circuit, in which case we expect that reaching the random Haar measure can also be realized in a circuit with  $\mathcal{O}(n \ln n)$  gates. It is already clear that this can be achieved if one uses the same 144 linear 3-bit (or 3-qubit) inflationary gates used above. We note that such a circuit would scramble in depth (or time)  $\mathcal{O}(\ln n)$ , matching the scrambling rate of a black hole [8–10, 12, 22, 23]. The remaining question is whether there is a random unstructured circuit of 2-qubit gates that can reach the same goal.

The second comment refers to the issue of averaging over circuits, which also connects to discussions of  $t$ -design (see [20, 31] and references therein). It is most instructive to consider an explicit example, namely that of the OTOC presented in Eq. (6), which measures the avalanche effect. For a given linear circuit [implemented by a linear permutation,  $P_j(x \oplus 2^i) = P_j(x) \oplus P_j(2^i) \oplus b_j$ , where  $b_j = 0, 1$ ],  $C_{\text{SAC}}^{ij} = (-1)^{P_j(2^i) \oplus b_j} = \pm 1$ . For a *single* realization of a random circuit, the  $\pm 1$  value of the correlator signals a weak cipher. By contrast, as discussed above, a good cipher must be built out of non-linear gates, in which case the correlator  $C_{\text{SAC}}^{ij}$  vanishes for a given (sufficiently large) circuit. It becomes immediately clear that if one averages over circuits at this stage, the difference between the linear and non-linear circuits is washed out. This points to the dangers of averaging too early, an issue well known from the theory of spin glasses [32, 33]. Learning from the latter, one should consider the behavior of a *typical* circuit by first squaring the correlator and only then averaging. This suggests an Edwards-Anderson-like order parameter,  $q_{\text{SAC}}^{ij} = \overline{(C_{\text{SAC}}^{ij})^2}$ , which is equal to 1 for linear circuits and vanishes for good ciphers. One can repeat this discussion in the context of quantum circuits, where averaging too early washes out the difference between Clifford and universal unitary gates. The vanishing of the average of the correlator  $C_{\text{SAC}}^{ij}$  is used to qualify Clifford circuits as 2-designs, a designation that is physically meaningless as it does not help one understand the behavior of a *typical* circuit. The difference between Clifford and universal quantum circuits becomes apparent if one uses the appropriate Edwards-Anderson-like order parameter, which in

the language of  $t$ -designs requires correlators with  $t \geq 4$ .

A related point, which follows from the discussions of delocalization of wave function amplitudes in string space, is that once the system is delocalized as signaled by the inverse participation ratio in Eq. (25), it is delocalized by any other measure: “Delocalized systems are all alike; every localized system is localized in its own way.” This suggests that once a system is a 4-design, it is also a  $t$ -design for  $t > 4$ .

The third and final comment is that one can extend the discussion of classical attacks expressed as OTOCs to quantum attacks [24]. In the latter, the trace involved in the computation of correlation functions (OTOCs) is replaced by projective measurements following the action of certain operations that can be translated into out-of-time-order operators (OTOOs), which we plan to explore

in a future publication.

In closing, our contribution to realizing fast ciphers with circuits of depth  $\mathcal{O}(\ln n)$  provides an exponential speed up in comparison to classic polynomial encryption algorithms, and should be of practical interest.

## ACKNOWLEDGMENTS

The authors would like to thank Shiyu Zhou and Luowen Qian for useful discussions at the early stages of this paper, and Ran Canetti for many enlightening conversations and for stimulating us to explore physics-inspired frameworks for quantifying scrambling by classical ciphers.

### Appendix A: Derivation of the OTOC in Eq. (7) that is associated to a CPCA on a 3-round Feistel cipher

Here we translate the attack presented by Patarin [14] on a 3-round Feistel cipher [see Sec. VB, in particular Eqs. (35) and (36), for notation] into an OTOC. The attack requires 3 oracle queries, 2 queries to the encryption oracle or  $P$ , and 1 query to the decryption oracle, or  $P^{-1}$ :

1. Choose an input  $(L_0^{(1)}, R_0^{(1)})$  and ask the encryption oracle for the output  $(L_3^{(1)}, R_3^{(1)}) = P(L_0^{(1)}, R_0^{(1)})$ ;
2. Choose  $L_0^{(2)} \neq L_0^{(1)}$  but reuse the same  $R_0^{(1)}$  value, and ask the encryption oracle for the output  $(L_3^{(2)}, R_3^{(2)}) = P(L_0^{(2)}, R_0^{(1)})$ ;
3. Ask the decryption oracle for  $(L_0^{(3)}, R_0^{(3)}) = P^{-1}(L_3^{(2)}, R_3^{(2)} \oplus L_0^{(1)} \oplus L_0^{(2)})$ .

For  $r = 3$ , one can show using Eqs. (35, 36) that  $R_0^{(3)} \oplus R_0^{(1)} \oplus L_3^{(2)} \oplus L_3^{(1)} = 0$ .

To construct an OTOC that expresses the above constraint, it suffices to use one bit,  $i$ , of the  $R$  register and one bit,  $j$ , of the  $L$  register. The correlation

$$\begin{aligned} C_{\text{CPCA}}^{ij} &= \text{tr} [\rho_\infty \hat{\sigma}_j^x(0) \hat{\sigma}_i^x(\tau) \hat{\sigma}_i^z(0) \hat{\sigma}_i^x(\tau) \hat{\sigma}_j^z(\tau) \hat{\sigma}_j^x(0) \hat{\sigma}_j^z(\tau) \hat{\sigma}_i^z(0)] \\ &= (-1)^{\delta_{ij}} \text{tr} \left[ \rho_\infty (\hat{\sigma}_i^z(0) \hat{\sigma}_i^x(\tau))^2 (\hat{\sigma}_j^z(\tau) \hat{\sigma}_j^x(0))^2 \right]. \end{aligned} \quad (\text{A1})$$

equals 1 if the evolution of the bit state is carried out via  $P$  and  $P^{-1}$ . The correspondence between the attack and the OTOC is extracted by following the sequence of operators from right-to-left in the first line of Eq. (A1):

1.  $\hat{\sigma}_i^z(0)$  measures bit  $i$  of  $x_i$ , or equivalently bit  $i - n/2$  of  $R_0^{(1)}$  ( $R$  occupies the second half of the  $n$ -bit long block), through  $(-1)^{x_i}$ , at the initial input state,  $|x\rangle = |(L_0^{(1)}, R_0^{(1)})\rangle$ ;
2.  $\hat{\sigma}_j^z(\tau)$  measures bit  $j$  of  $L_3^{(1)}$ , through  $(-1)^{P_j(x)}$ , at the output and returns the system to the initial input state,  $|x\rangle$ ;
3.  $\hat{\sigma}_j^x(0)$  flips the  $j$ -th bit of the initial input state,  $|x\rangle$ , into  $|x \oplus 2^j\rangle$ , thus setting  $L_0^{(2)} = L_0^{(1)} \oplus 2^j$ ;
4.  $\hat{\sigma}_i^x(\tau) \hat{\sigma}_j^z(\tau)$  first measures bit  $j$  of  $L_3^{(2)}$ ,  $(-1)^{P_j(x \oplus 2^j)}$ , at the output, then flips the  $i$ -th of the output state, thus shifting  $R_3^{(2)} \rightarrow R_3^{(2)} \oplus 2^{i-n/2}$ , and subsequently evolves the system backwards (via the  $P^{-1}$ ) to the state  $|(L_0^{(3)}, R_0^{(3)})\rangle$ ;
5.  $\hat{\sigma}_i^z(0)$  measures bit  $i - n/2$  of  $R_0^{(3)}$ ; and finally,

6. the product  $\hat{\sigma}_j^x(0) \hat{\sigma}_i^x(\tau)$  undoes the flips above to restore the state to  $|x\rangle$ , so as to express the result as a trace over all possible inputs.

The correlator Eq. (A1) thus returns the average over inputs of  $(-1)^{[R_0^{(3)}]_{i-n/2}+[R_0^{(1)}]_{i-n/2}+[L_3^{(2)}]_j+[L_3^{(1)}]_j}$ ; given the condition that  $R_0^{(3)} \oplus R_0^{(1)} \oplus L_3^{(2)} \oplus L_3^{(1)} = 0$  for a 3-round Feistel cipher, it follows that

$$C_{\text{CPCA}}^{i=j+n/2 \ j} = 1. \quad (\text{A2})$$

We have therefore successfully translated the attack on the 3-round Feistel cipher in Ref. [14] into an OTOC.

### Appendix B: Avalanche OTOC in terms of string amplitudes

Let us consider the OTOC presented in Eq. (6) that quantifies the avalanche effect. We shall use the general expression Eq. (16), with  $\hat{S}_\alpha = \hat{\sigma}_i^x$  and  $\hat{S}_\beta = \hat{\sigma}_j^z$ . We write the OTOC in terms of the string space amplitudes:

$$\begin{aligned} C_{\text{SAC}}^{ij} &= \sum_{\gamma_1, \gamma_2} A_{\beta\gamma_1}(\tau) A_{\beta\gamma_2}(\tau) \text{tr} \left[ \rho_\infty \hat{S}_\alpha \hat{S}_{\gamma_1} \hat{S}_\alpha \hat{S}_{\gamma_2} \right] \\ &= \sum_{\gamma} |A_{\beta\gamma}(\tau)|^2 (-1)^{\gamma^z \cdot \alpha^x} (-1)^{\gamma^z \cdot \gamma^x}. \end{aligned} \quad (\text{B1})$$

We use that the parity of  $n_y(\gamma) = \gamma^z \cdot \gamma^x$  is a conserved quantity, and thus  $n_y(\gamma) = n_y(\beta) = 0$  for all the  $\gamma$  such that  $A_{\beta\gamma}(\tau) \neq 0$ , which allows us to drop the  $(-1)^{\gamma^z \cdot \gamma^x}$  in the last line of Eq. (B1). Also,  $\gamma^z \cdot \gamma^x = 0$  if  $\hat{\sigma}_i^z \notin \hat{S}_\gamma$  and  $\gamma^z \cdot \gamma^x = 1$  if  $\hat{\sigma}_i^z \in \hat{S}_\gamma$ . We can thus write

$$\begin{aligned} C_{\text{SAC}}^{ij} &= \sum_{\gamma | \hat{\sigma}_i^z \notin \hat{S}_\gamma} |A_{\beta\gamma}(\tau)|^2 - \sum_{\gamma | \hat{\sigma}_i^z \in \hat{S}_\gamma} |A_{\beta\gamma}(\tau)|^2 \\ &= \sum_{\gamma | \hat{\sigma}_i^z \notin \hat{S}_\gamma} |A_{\gamma\beta}(-\tau)|^2 - \sum_{\gamma | \hat{\sigma}_i^z \in \hat{S}_\gamma} |A_{\gamma\beta}(-\tau)|^2, \end{aligned} \quad (\text{B2})$$

where we used the time-reversal relation Eq. (20) in going from the first to the second line. Notice that the two terms in the last line of Eq. (B2) correspond to the probabilities  $p_{0|\beta}$  and  $p_{z|\beta}$ , respectively, that the strings contain either an identity or a  $\hat{\sigma}^z$  operator at position  $i$ , given the initial string  $\beta$  that contains identities at all locations except for location  $j$ . We thus arrive at the expression shown in Eq. (45).

### Appendix C: Inflationary gates

In the table below we list all the permutations in  $S_8$  that are associated to the 144 inflationary gates. These 3-bit gates are all linear, and can be expressed in a circuit equivalent with 2-bit CNOT gates as exemplified in Fig. C.1.

1: 03567421	25: 14637205	49: 25701643	73: 41273650	97: 52340761	121: 63145027
2: 03657412	26: 14726305	50: 25704316	74: 41362750	98: 52346107	122: 63501427
3: 03745621	27: 16254370	51: 27145063	75: 41367205	99: 52610734	123: 65031274
4: 03746512	28: 16257043	52: 27415036	76: 41723605	100: 52613407	124: 65120374
5: 05367241	29: 16432570	53: 27501463	77: 42173560	101: 53062471	125: 65123047
6: 05637214	30: 16437025	54: 27504136	78: 42351760	102: 53240671	126: 65301247
7: 05723641	31: 16702543	55: 30475621	79: 42357106	103: 53246017	127: 70162543
8: 05726314	32: 16704325	56: 30476512	80: 42713506	104: 53602417	128: 70164325
9: 06357142	33: 17246053	57: 30564721	81: 43162570	105: 56032174	129: 70251643
10: 06537124	34: 17426035	58: 30654712	82: 43167025	106: 56210374	130: 70254316
11: 06713542	35: 17602453	59: 34075261	83: 43251670	107: 56213047	131: 70431625
12: 06715324	36: 17604235	60: 34076152	84: 43257016	108: 56302147	132: 70432516
13: 07345261	37: 21475630	61: 34520761	85: 43701625	109: 60173542	133: 71062453
14: 07346152	38: 21564730	62: 34526107	86: 43702516	110: 60175324	134: 71064235
15: 07523461	39: 21567403	63: 34610752	87: 47123065	111: 60351742	135: 71240653
16: 07526134	40: 21745603	64: 34615207	88: 47213056	112: 60531724	136: 71420635
17: 07613452	41: 24175360	65: 35064271	89: 47301265	113: 61073452	137: 72051463
18: 07615234	42: 24531760	66: 35420671	90: 47302156	114: 61075234	138: 72054136
19: 12476530	43: 24537106	67: 35426017	91: 50273641	115: 61340752	139: 72140563
20: 12654730	44: 24715306	68: 35604217	92: 50276314	116: 61345207	140: 72410536
21: 12657403	45: 25164370	69: 36054172	93: 50362741	117: 61520734	141: 74031265
22: 12746503	46: 25167043	70: 36410572	94: 50632714	118: 61523407	142: 74032156
23: 14276350	47: 25431670	71: 36415027	95: 52073461	119: 63051472	143: 74120365
24: 14632750	48: 25437016	72: 36504127	96: 52076134	120: 63140572	144: 74210356

TABLE OF INFLATIONARY GATES. The lists of 8 numbers correspond to the outputs for each of the inputs 0 1 2 3 4 5 6 7, i.e., the corresponding permutation list. These 144 gates are found as follows. We compute the entries  $t_{\alpha'\alpha}^{(g)}$  of the  $64 \times 64$  transition in Eq. (41) for each of the  $8!$  gates in  $S_8$ . We filter out all gates for which the  $9 \times 9$  submatrix connecting the 9-dimensional subspace of weight 1 strings is non-zero, thus retaining only gates for which weight 1 substrings grow into weight 2 or 3 substrings. All these gates are linear.

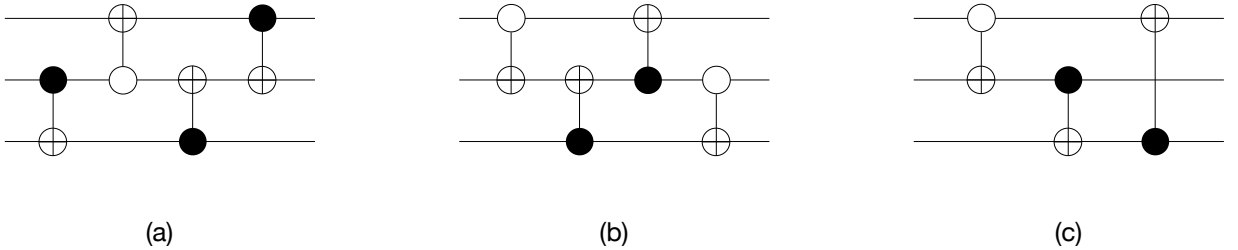


FIG. C.1. Examples of 3 circuits written with 2-bit CNOT gates that are equivalent to the inflationary 3-bit gates. There are  $3 \times 2^4 = 48$  circuits with the topology of the example shown in (a), where the factor of 3 counts the number of ways of choosing the bit line with two controls and the factor of  $2^4$  counts the choices of negated or not control (white or black control). Similarly, there are  $3 \times 2^4 = 48$  circuits with the topology of (b). Finally, there are  $3! \times 2^3 = 48$  circuits similar to (c). In total, there are 144 such circuits.

- [1] S. Goldwasser and M. Bellare, “Lecture notes on cryptography,” Chap. 4, (2001).
- [2] Michael Luby and Charles Rackoff, “How to construct pseudorandom permutations from pseudorandom functions,” *SIAM Journal on Computing* **17**, 373–386 (1988), <https://doi.org/10.1137/0217022>.
- [3] Don Coppersmith and Edna Grossman, “Generators for certain alternating groups with applications to cryptography,” *SIAM Journal on Applied Mathematics* **29**, 624–627 (1975).
- [4] Shlomo Hoory, Avner Magen, Steven Myers, and Charles Rackoff, “Simple permutations mix well,” *Theoretical Computer Science* **348**, 251–261 (2005).
- [5] A. Brodsky and S. Hoory, “Simple permutations mix even better,” *Random Struct. Algorithms* **32**, 274–289 (2008).
- [6] A. I. Larkin and Yu. N. Ovchinnikov, “Quasiclassical method in the theory of superconductivity,” *Soviet Journal of Experimental and Theoretical Physics* **28**, 1200 (1969).
- [7] A Kitaev, “Hidden Correlations in the Hawking Radiation and Thermal Noise, talk given at KITP, Santa Barbara,” <http://online.kitp.ucsb.edu/online/joint98/kitaev/> (2014).
- [8] Stephen H. Shenker and Douglas Stanford, “Black holes and the butterfly effect,” *Journal of High Energy Physics* **2014** (2014), 10.1007/jhep03(2014)067.
- [9] Stephen H. Shenker and Douglas Stanford, “Multiple shocks,” *Journal of High Energy Physics* **2014** (2014), 10.1007/jhep12(2014)046.
- [10] Juan Maldacena, Stephen H. Shenker, and Douglas Stanford, “A bound on chaos,” *Journal of High Energy Physics* **2016** (2016), 10.1007/jhep08(2016)106.
- [11] Igor L. Aleiner, Lara Faoro, and Lev B. Ioffe, “Microscopic model of quantum butterfly effect: Out-of-time-order correlators and traveling combustion waves,” *Annals of Physics* **375**, 378 – 406 (2016).
- [12] Douglas Stanford, “Many-body chaos at weak coupling,” *Journal of High Energy Physics* **2016** (2016), 10.1007/jhep10(2016)009.
- [13] F. Wegner, “Inverse participation ratio in  $2+\epsilon$  dimensions,” *Zeitschrift für Physik B Condensed Matter and Quanta* **36**, 209–214 (1980).
- [14] Jacques Patarin, “Generic attacks on Feistel schemes,” in *Advances in Cryptology — ASIACRYPT 2001*, edited by Colin Boyd (Springer Berlin Heidelberg, Berlin, Heidelberg, 2001) pp. 222–238.
- [15] R. Oliveira, O. C. O. Dahlsten, and M. B. Plenio, “Generic entanglement can be generated efficiently,” *Physical Review Letters* **98** (2007), 10.1103/physrevlett.98.130502.
- [16] Aram W. Harrow and Richard A. Low, “Random quantum circuits are approximate 2-designs,” *Communications in Mathematical Physics* **291**, 257–302 (2009).
- [17] Winton Brown and Omar Fawzi, “Scrambling speed of random quantum circuits,” (2013), arXiv:1210.6644 [quant-ph].
- [18] Winton Brown and Omar Fawzi, “Decoupling with random quantum circuits,” *Communications in Mathematical Physics* **340**, 867–900 (2015).
- [19] Fernando G. S. L. Brandão, Aram W. Harrow, and Michał Horodecki, “Local random quantum circuits are approximate polynomial-designs,” *Communications in Mathematical Physics* **346**, 397–434 (2016).
- [20] Aram Harrow and Saeed Mehraban, “Approximate unitary  $t$ -designs by short random quantum circuits using nearest-neighbor and long-range gates,” (2018), arXiv:1809.06957 [quant-ph].
- [21] F. Arute, K. Arya, R. Babbush, D. Bacon, J. C. Bardin, R. Barends, R. Biswas, S. Boixo, F. G. S. L. Brandao, D. A. Buell, B. Burkett, Y. Chen, Z. Chen, B. Chiaro, R. Collins, W. Courtney, A. Dunsworth, E. Farhi, B. Foxen, A. Fowler, C. Gidney, M. Giustina, R. Graff, K. Guerin, S. Habegger, M. P. Harrigan, M. J. Hartmann, A. Ho, M. Hoffmann, T. Huang, T. S. Humble, S. V. Isakov, E. Jeffrey, Z. Jiang, D. Kafri, K. Kechedzhi, J. Kelly, P. V. Klimov, S. Knysh, A. Korotkov, F. Kostritsa, D. Landhuis, M. Lindmark, E. Lucero, D. Lyakh, S. Mandrà, J. R. McClean, M. McEwen, A. Megrant, X. Mi, K. Michielsen, M. Mohseni, J. Mutus, O. Naaman, M. Neeley, C. Neill, M. Yuezhen Niu, E. Ostby, A. Petukhov, J. C. Platt, C. Quintana, E. G. Rieffel, P. Roushan, N. C. Rubin, D. Sank, K. J. Satzinger, V. Smelyanskiy, K. J. Sung, M. D. Trevithick, A. Vainsencher, B. Villalonga, T. White, Z. Jamie Yao, P. Yeh, A. Zalcman, H. Neven, and J. M. Martinis, “Quantum supremacy using a programmable superconducting processor,” *Nature* **574**, 505–510 (2019).
- [22] Patrick Hayden and John Preskill, “Black holes as mirrors: quantum information in random subsystems,” *Journal of High Energy Physics* **2007**, 120–120 (2007).
- [23] Yasuhiro Sekino and L Susskind, “Fast scramblers,” *Journal of High Energy Physics* **2008**, 065–065 (2008).
- [24] Gembu Ito, Akinori Hosoyamada, Ryutaroh Matsumoto, Yu Sasaki, and Tetsu Iwata, “Quantum chosen-ciphertext attacks against feistel ciphers,” in *Topics in Cryptology – CT-RSA 2019*, edited by Mitsuru Matsui (Springer International Publishing, Cham, 2019) pp. 391–411.
- [25] Edward Fredkin and Tommaso Toffoli, “Conservative logic,” *International Journal of Theoretical Physics* **21**, 219–253 (1982).
- [26] Horst Feistel, “Cryptography and computer privacy,” *Scientific American* **228**, 15–23 (1973).
- [27] Sheelagh Lloyd, “Eurocrypt 90: Proceedings of the workshop on the theory and application of cryptographic techniques on advances in cryptology,” (Springer-Verlag, Berlin, Heidelberg, 1991).
- [28] Hirose Shouichi and Ikeda Katsuo, “Nonlinearity criteria of boolean functions,” (1995).
- [29] Daniel Gottesman, “The Heisenberg Representation of Quantum Computers,” in *Proceedings of the XXII International Colloquium on Group Theoretical Methods in Physics*, eds. S. P. Corney, R. Delbourgo, and P. D. Jarvis (International Press, 1999) pp. 32–43.
- [30] Scott Aaronson and Daniel Gottesman, “Improved simulation of stabilizer circuits,” *Physical Review A* **70** (2004), 10.1103/physreva.70.052328.
- [31] Daniel A. Roberts and Beni Yoshida, “Chaos and complexity by design,” *Journal of High Energy Physics* **2017** (2017), 10.1007/jhep04(2017)121.
- [32] K. H. Fischer and J. A. Hertz, *Spin glasses*, 1st ed., Cam-

- bridge Studies in Magnetism (Cambridge Univ. Press, Cambridge, 1993).
- [33] S F Edwards and P W Anderson, “Theory of spin glasses,” *Journal of Physics F: Metal Physics* **5**, 965–974 (1975).